

Classical Notions and Problems in Thurston Geometries

Jenő Szirmai

(Communicated by Kazim Ilarslan)

ABSTRACT

Of the Thurston geometries, those with constant curvature geometries (Euclidean E^3 , hyperbolic H^3 , spherical S^3) have been extensively studied, but the other five geometries, $H^2 \times R$, $S^2 \times R$, Nil, \widetilde{SL}_2R , Sol have been thoroughly studied only from a differential geometry and topological point of view. However, classical concepts highlighting the beauty and underlying structure of these geometries – such as geodesic curves and spheres, the lattices, the geodesic triangles and their surfaces, their interior sum of angles and similar statements to those known in constant curvature geometries – can be formulated. These have not been the focus of attention. In this survey, we summarize our results on this topic and pose additional open questions.

Keywords: Thurston geometries, geodesic curves, geodesic triangles, spheres, sphere packings and coverings, lattices.

AMS Subject Classification (2020): Primary: 53A20; Secondary: 53A35; 52C17; 52C22; 52B15; 57M12; 57M25; 52C35; 53B20.

1. Introduction

W. Thurston's results are essential for understanding the geometric structure of our world, where the eight so-called Thurston geometries play the leading role. The importance of these geometries is emphasized by Thurston's famous theorem:

Let $(X; G)$ be a 3-dimensional homogeneous geometry, where X is a simply connected Riemannian space with a maximal group G of isometries, acting transitively on X with compact point stabilizers. G is maximal means that no proper extension of G can act on the Riemannian space X in the same way. We recall the

Theorem 1.1 (Thurston, [54, 80]). *Any 3-dimensional homogeneous geometry $(X; G)$ that admits a compact quotient is equivalent (equivariant) to one of the geometries $(X; G) = Isom(X)$ where the space X is one of E^3 , H^3 , S^3 , $H^2 \times R$, $S^2 \times R$, Nil, \widetilde{SL}_2R or Sol.*

Therefore, there are eight so-called Thurston geometries, described in [54, 80]. Among them E^3 , S^3 and H^3 are the classical spaces of constant zero, positive and negative curvature, respectively. Further geometries $S^2 \times R$, $H^2 \times R$ denote the direct product geometries where S^2 is the spherical and H^2 is the hyperbolic base plane and the real line R is with usual metric. Then \widetilde{SL}_2R and Nil are obtained as twisted products of R with H^2 and E^2 , respectively; and finally Sol geometry is a twisted product of the Minkowski plane M^2 as fibre, with R as base. In each of them there exists an infinitesimal (positive definite) Riemannian metric that is invariant under certain translations, guaranteeing homogeneity at every point. These translations in general commute only in E^3 , but a discrete (discontinuous) translation group, taken as a lattice, can be defined with compact fundamental domain in analogy to the Euclidean case, but with some different properties. The additional symmetries can define crystallographic groups, giving nice tilings, packings, material structures, etc.

Received : 20-12-2022, Accepted : 11-07-2023

* Corresponding author

Dedicated to Professor Emil Molnár on the occasion of his 80th birthday

I mention here only the packing and covering problems. In addition to pure mathematical curiosity, the study of sphere packings and coverings *generalized Kepler problem* is important because it is possible that under different conditions (e.g. strong magnetic field) materials cannot be realized in the usual Euclidean space but in one of the other Thurston geometries. The structures of substances formed under these conditions may differ from the Euclidean case and can follow, for example, the geometry of non-constant curvature spaces, and in these new geometries their atoms can be modeled by $\mathbf{H}^2 \times \mathbf{R}$, $\mathbf{S}^2 \times \mathbf{R}$, Nil, $\widetilde{\mathbf{SL}}_2\mathbf{R}$ or Sol spheres. For example, in Nil geometry we can define lattices and corresponding lattice-like ball packings where we found geodesic ball packings with kissing number 14 that is denser than the densest Euclidean case (see Section 7, [34], [55]). (The density is ≈ 0.78085).

A unified approach to Thurston geometries enabling the investigations in this direction were made possible by the nice paper of E. Molnár [30] where he showed that the Thurston geometries can be uniformly modeled in the projective 3-space \mathcal{P}^3 (or in the projective 3-sphere \mathcal{PS}^3). The projective spherical model is based on linear algebra over the real vector space \mathbf{V}^4 (for points) and its dual \mathbf{V}_4 (for planes), up to a positive real factor, so that the proper dimension is indeed three. A plane \rightarrow point polarity or scalar product (by specified signature) induces the invariant metric in a unified way. In our work we will use these projective models of Thurston geometries.

The constant curvature geometries \mathbf{E}^3 , \mathbf{H}^3 , \mathbf{S}^3 have been extensively studied from the point of view of elementary geometry, differential geometry and topology. In this article we focus on results obtained in the other five non-constant curvature Thurston geometries $\mathbf{H}^2 \times \mathbf{R}$, $\mathbf{S}^2 \times \mathbf{R}$, Nil, $\widetilde{\mathbf{SL}}_2\mathbf{R}$, Sol. These spaces have been investigated from the perspective of differential geometry and topology but few results are stated in connection with their internal structure in the classical sense. A lot of elementary notions are missing, problems are not formulated, theorems are not proved. Hence, in this survey we focus on non-constant curvature Thurston geometries and we emphasize some surprising facts.

Now, we review the notions of distance, angle, sphere, geodesic triangle, their surfaces and congruences in each aforementioned geometry. Then we survey Apollonius surfaces, Dirichlet–Voronoi cells, and in a separate chapter we review the concepts of sphere (ball) packings and their densities and the corresponding results so far.

Furthermore, we emphasize the results related to the projective models of the considered geometries. In our opinion, these models are suitable for the elementary examination and visualization of the above geometries.

Remark 1.2. There is another way of defining distance using the concept of so-called translational distance. We introduced this concept in the paper [32], but in this survey we summarize the results related to the concept of geodesic distance. Note that translation distance and geodesic distance are the same in the Euclidean geometry \mathbf{E}^3 , Bolyai–Lobachevsky hyperbolic geometry \mathbf{H}^3 , spherical $\mathbf{S}^2 \times \mathbf{R}$ and $\mathbf{H}^2 \times \mathbf{R}$ spaces, but give different values in the Nil, Sol and $\widetilde{\mathbf{SL}}_2\mathbf{R}$ geometries (see [7, 37, 39, 60, 57, 64, 81]).

As the reader will see, the above results and their visualizations will open a new window towards other (geometric) worlds.

2. On the projective models of Thurston geometries

We first summarize the key information about projective models of Thurston geometries (see [30, 31, 34]).

All the Thurston 3-geometries will be uniformly modelled in the *projective spherical space* \mathcal{PS}^3 that can be embedded into the affine hence into *Euclidean 4-space*. Our main tool will be a 4-dimensional vector space \mathbf{V}^4 over the real numbers \mathbf{R} with basis $\{\mathbf{e}_0, \mathbf{e}_1, \mathbf{e}_2, \mathbf{e}_3\}$ (that is not assumed to be orthonormal).

\mathbf{V}^4 is the embedding real vector space with its affine image $\mathcal{A}^4(O, \mathbf{V}^3, \mathbf{V}_3)$. Let $\{O; \mathbf{e}_0, \mathbf{e}_1, \mathbf{e}_2, \mathbf{e}_3\}$, be a *coordinate system* in the affine 4-space $\mathcal{A}^4 = \mathbf{E}^4$ with origin O and a (not necessarily orthonormal) vector basis $\{\mathbf{e}_0, \mathbf{e}_1, \mathbf{e}_2, \mathbf{e}_3\}$ for \mathbf{V}^4 , where our affine model plane $\mathcal{A}^3 = \mathbf{E}^3 \subset \mathcal{P}^3 = \mathcal{A}^3 \cup (i)$ is placed to the point $E_0(\mathbf{e}_0)$ with equation $x^0 = 1$. Here any non-zero vector $\mathbf{x} = x^0\mathbf{e}_0 + x^1\mathbf{e}_1 + x^2\mathbf{e}_2 + x^3\mathbf{e}_3 =: x^i\mathbf{e}_i$ (the index sum convention of Einstein–Schouten will be used) represents a point $X(\mathbf{x})$ of \mathcal{A}^3 , but also a point of the *projective sphere* \mathcal{PS}^3 after having introduced the following *positive equivalence*. For non-zero vectors

$$\begin{aligned} \mathbf{x} &\sim c \mathbf{x} \text{ with } 0 < c \in \mathbf{R} \text{ represent the same point } X = (\mathbf{x} \sim c \mathbf{x}) \text{ of } \mathcal{PS}^3; \\ \mathbf{z} &\sim 0 \mathbf{e}_0 + z^1\mathbf{e}_1 + z^2\mathbf{e}_2 + z^3\mathbf{e}_3 \text{ will be an ideal point } (z) \text{ of } \mathcal{PS}^3. \end{aligned} \tag{2.1}$$

We write $(z) \in (i)$, where (i) is the ideal plane (sphere) to \mathcal{A}^3 , extending the affine space \mathcal{A}^3 into the projective sphere \mathcal{PS}^3 . Here (z) and $(-z)$, and in general (\mathbf{x}) and $(-\mathbf{x})$, are opposite points of \mathcal{PS}^3 . Then the *identification*

of the opposite point pairs of \mathcal{PS}^3 leads to the projective space \mathcal{P}^3 . Thus the embedding $\mathcal{A}^3 = \mathbf{E}^3 \subset \mathcal{P}^3 \subset \mathcal{PS}^3$ can be formulated in the vector space \mathbf{V}^3 in a unified way.

The dual (form) space \mathbf{V}_4 to \mathbf{V}^4 is defined as the set of *real valued linear functionals* or forms on \mathbf{V}^4 . This means that we pose the following requirements for any form $\mathbf{u} \in \mathbf{V}_3$

$$\begin{aligned} \mathbf{u} : \mathbf{V}^4 \ni \mathbf{x} &\mapsto \mathbf{x}\mathbf{u} \in \mathbf{R} \text{ with linearity} \\ (\mathbf{ax} + \mathbf{by})\mathbf{u} &= a(\mathbf{x}\mathbf{u}) + b(\mathbf{y}\mathbf{u}) \text{ for any } \mathbf{x}, \mathbf{y} \in \mathbf{V}^4 \text{ and for any } a, b \in \mathbf{R}. \end{aligned} \quad (2.2)$$

We emphasize our convention. *The vector coefficients are written from the left, then linear forms act on vectors on the right (as an easy associativity law; similar conventions will be used also later on).*

This "built in" linear structure allows us to define the addition $\mathbf{u} + \mathbf{v}$ of two linear forms \mathbf{u}, \mathbf{v} , and the multiplication \mathbf{uc} of a linear form \mathbf{u} by a real factor c , both resulting in linear forms of \mathbf{V}_4 . Moreover, we can define for any basis $\{\mathbf{e}_i\}$ in \mathbf{V}^4 the *dual basis* $\{\mathbf{e}^j\}$ in \mathbf{V}_4 by the Kronecker symbol δ_i^j :

$$\mathbf{e}_i \mathbf{e}^j = \delta_i^j = \begin{cases} 1 & \text{if } i = j \\ 0 & \text{if } i \neq j \end{cases} \quad i, j = 0, 1, 2, 3. \quad (2.3)$$

Furthermore, we see that the general linear form $\mathbf{u} := e^0 u_0 + e^1 u_1 + e^2 u_2 + e^3 u_3 := e^j u_j$ takes on the vector $\mathbf{x} := x^0 \mathbf{e}_0 + x^1 \mathbf{e}_1 + x^2 \mathbf{e}_2 + x^3 \mathbf{e}_3 := x^i \mathbf{e}_i$ the real value

$$(x^i \mathbf{e}_i)(\mathbf{e}^j u_j) = x^i (\mathbf{e}_i \mathbf{e}^j) u_j = x^i \delta_i^j u_j = x^i u_i := x^0 u_0 + x^1 u_1 + x^2 u_2 + x^3 u_3. \quad (2.4)$$

Thus, a linear form $\mathbf{u} \in \mathbf{V}_4$ describes a *3-dimensional subspace* u , i.e., a vector hyperplane of \mathbf{V}^4 through the origin. Moreover, forms

$$\mathbf{u} \sim \mathbf{uk} \text{ with } 0 < k \in \mathbf{R} \text{ represent the same oriented hyperplane of } \mathbf{V}^4. \quad (2.5)$$

The positive equivalence class of forms (\mathbf{u}) determines an open *half-space* $(\mathbf{u})^+$ of \mathbf{V}^4 , i.e., the vector classes (\mathbf{x}) for which

$$(\mathbf{u})^+ := \{(\mathbf{x}) : \mathbf{x}\mathbf{u} > 0\}. \quad (2.6)$$

This also gives a corresponding half-sphere of \mathcal{PS}^3 , and a corresponding half-hyperplane of \mathcal{A}^3 . Note that *this is not so for the projective plane* \mathcal{P}^2 which is not orientable, because the equivalence mapping $\mathbf{x} \mapsto -\mathbf{x}$ has negative determinant in \mathbf{V}^4 !

In order to advance on our main goal, we introduce a *bijective linear mapping* \mathbf{T} of \mathbf{V}^4 onto itself, i.e.

$$\begin{aligned} \mathbf{T} : \mathbf{V}^3 \ni \mathbf{x} &\mapsto \mathbf{x}\mathbf{T} =: \mathbf{y} \in \mathbf{V}^3 \text{ with requirements} \\ x^i \mathbf{e}_i &\mapsto (x^i \mathbf{e}_i)\mathbf{T} = x^i (\mathbf{e}_i \mathbf{T}) = x^i t_i^j \mathbf{e}_j =: y_j \mathbf{e}_j, \det(t_i^j) \neq 0. \end{aligned} \quad (2.7)$$

Assume that \mathbf{T} has the above matrix (t_i^j) with respect to basis $\{\mathbf{e}_i\}$ of \mathbf{V}^3 ($i, j = 0, 1, 2$). Then \mathbf{T} defines a *projective point transformation* $\tau(\mathbf{T})$ of \mathcal{PS}^2 onto itself, which *preserves all the incidences of subspaces of* \mathbf{V}^3 and hence *incidences of points and lines of* \mathcal{PS}^2 , respectively. The matrix (t_i^j) and its positive multiples $(ct_i^j) = (t_i^j c)$ with $0 < c \in \mathbf{R}$ (and only these mappings) define the same point transformation $\tau(\mathbf{T} \sim \mathbf{T}c)$ of \mathcal{PS}^2 by the above requirements. As usual, we define the composition, or product, of transforms \mathbf{T} and \mathbf{W} of vector space \mathbf{V}^3 in this order (right action on \mathbf{V}^3) by

$$\mathbf{T}\mathbf{W} : \mathbf{V}^4 \ni \mathbf{x} \rightarrow (\mathbf{x}\mathbf{T})\mathbf{W} = \mathbf{y}\mathbf{W} = \mathbf{z} =: \mathbf{x}(\mathbf{T}\mathbf{W}) \quad (2.8)$$

with matrices (t_i^j) and (w_j^k) to basis $\{\mathbf{e}_i\}$ ($i, j, k = 0, 1, 2, 3$) as follows by our index conventions:

$$\mathbf{e}_i(\mathbf{T}\mathbf{W}) = (\mathbf{e}_i \mathbf{T})\mathbf{W} = (t_i^j \mathbf{e}_j)\mathbf{W} = (t_i^j)(w_j^k \mathbf{e}_k) = (t_i^j w_j^k) \mathbf{e}_k, \quad (2.9)$$

with summation (from 0 to 3) for the occurring equal upper and lower indices.

The above *inverse matrix class* (t_i^j) is denoted by $(T_j^k) \sim \frac{1}{c} T_j^k$, with $t_i^j T_j^k = \delta_i^k$ inducing the corresponding linear transform \mathbf{T} of the dual \mathbf{V}_4 (i.e. for lines) onto itself, and its inverse \mathbf{T}^{-1} , i.e.,

$$\begin{aligned} \mathbf{T} : \mathbf{V}^4 \ni \mathbf{v} &\mapsto \mathbf{T}\mathbf{v} =: \mathbf{u} \in \mathbf{V}_4 \text{ such that} \\ \mathbf{y}\mathbf{v} &= (\mathbf{x}\mathbf{T})\mathbf{v} = \mathbf{x}(\mathbf{T}\mathbf{v}) = \mathbf{x}\mathbf{u}, \text{ specifically} \\ 0 = \mathbf{x}\mathbf{u} &= (\mathbf{x}\mathbf{T})(\mathbf{T}^{-1}\mathbf{u}) = \mathbf{y}\mathbf{v}, \text{ so } 0 = \mathbf{y}\mathbf{v} = (\mathbf{y}\mathbf{T}^{-1})(\mathbf{T}\mathbf{v}) = \mathbf{x}\mathbf{u} \\ X \text{ I } u &\leftrightarrow Y := X \tau \text{ I } v := \tau u \text{ holds (see (2.13))} \end{aligned} \quad (2.10)$$

for the τ -images of points and lines, respectively. We can see that the induced action on the dual V_3 is a *left action* and so is the induced action on the lines of \mathcal{PS}^2 .

Let us introduce the positive equivalence in V^4 for non-zero vectors

$$\mathbf{x} \sim c \mathbf{x} \text{ with } 0 < c \in \mathbf{R} \text{ defines the same point } X(\mathbf{x}) \text{ of } \mathcal{PS}^3 \tag{2.11}$$

whose coordinates in $\mathbf{x} = x^i \mathbf{e}_i$, with respect to basis $\{\mathbf{e}_i\}$ ($i = 0, 1, 2, 3$), can be written in matrix form

$$\mathbf{x} = (x^0, x^1, x^2, x^3) \begin{pmatrix} \mathbf{e}_0 \\ \mathbf{e}_1 \\ \mathbf{e}_2 \\ \mathbf{e}_3 \end{pmatrix}. \text{ A form } \mathbf{u} = (e^0 \ e^1 \ e^2 \ e^3) \begin{pmatrix} u_0 \\ u_1 \\ u_2 \\ u_3 \end{pmatrix} \tag{2.12}$$

in the dual space V_4 , again up to positive equivalence, describes an oriented plane (2-sphere) of \mathcal{PS}^3 with the dual basis $\{\mathbf{e}^j\}$, $\mathbf{e}_i \mathbf{e}^j = \delta_i^j$ (the Kronecker symbol) ($i, j = 0, 1, 2, 3$). Equalities

$$0 = (x^i \mathbf{e}_i)(\mathbf{e}^j u_j) = x^i (\mathbf{e}_i \mathbf{e}^j) u_j = x^i \delta_i^j u_j = x^i u_i \tag{2.13}$$

express the incidence $X \perp u$. Formula (2.13) describes the set of varying points $X(\mathbf{x})$ on the fixed plane $u(\mathbf{u})$, and at the same time the set of planes $u(\mathbf{u})$ incident to the fixed point $X(\mathbf{x})$. The projective transform $\tau(\mathbf{T}, \mathbf{T}^{-1})$ with inverse matrix pair (t_i^j) to \mathbf{T} of V^4 and $(t_j^i)^{-1} \sim (T_j^k)$ to \mathbf{T}^{-1} of V_4 – with respect to the dual basis pair $\{\mathbf{e}_i\}$, $\{\mathbf{e}^j\}$, as in formulas (2.10) – can be described in matrix form. First for points it is:

$$(x^0, x^1, x^2, x^3) \begin{pmatrix} t_0^0 & t_0^1 & t_0^2 & t_0^3 \\ t_1^0 & t_1^1 & t_1^2 & t_1^3 \\ t_2^0 & t_2^1 & t_2^2 & t_2^3 \\ t_3^0 & t_3^1 & t_3^2 & t_3^3 \end{pmatrix} \begin{pmatrix} \mathbf{e}_0 \\ \mathbf{e}_1 \\ \mathbf{e}_2 \\ \mathbf{e}_3 \end{pmatrix} \sim (y^0, y^1, y^2, y^3) \begin{pmatrix} \mathbf{e}_0 \\ \mathbf{e}_1 \\ \mathbf{e}_2 \\ \mathbf{e}_3 \end{pmatrix} \tag{2.14}$$

and for planes $e^i T_i^k u_k \sim e^i v_i$. Here $\tau(\mathbf{T}, \mathbf{T}^{-1})$ preserves the incidence by $0 = (\mathbf{x}\mathbf{u}) = (\mathbf{y}\mathbf{v})$. These are, again up to positive equivalence, related to a coordinate simplex $E_0 E_1 E_2 E_3$ with the unit point $E(\mathbf{e} = \mathbf{e}_0 + \mathbf{e}_1 + \mathbf{e}_2 + \mathbf{e}_3)$ and to $e^0 e^1 e^2 e^3$ with the unit plane $e(\mathbf{e} = e^0 + e^1 + e^2 + e^3)$, where $e^i = (E_j E_k E_l)$ with $\{0, 1, 2, 3\} = \{i, j, k, l\}$.

Spherical space geometry \mathbf{S}^3 is defined with the additional polarity $\Pi(\ast)$ or scalar product \langle , \rangle in V_4 , with positive diagonal matrix (π^{ij}) and we have $\mathbf{e}_\ast^i = \mathbf{e}^i = \pi^{ij} \mathbf{e}_j$,

$$(\mathbf{e}^0, \mathbf{e}^1, \mathbf{e}^2, \mathbf{e}^3) \xrightarrow{\ast} \begin{pmatrix} \mathbf{e}^0 \\ \mathbf{e}^1 \\ \mathbf{e}^2 \\ \mathbf{e}^3 \end{pmatrix} = \begin{pmatrix} 1 & 0 & 0 & 0 \\ 0 & 1 & 0 & 0 \\ 0 & 0 & 1 & 0 \\ 0 & 0 & 0 & 1 \end{pmatrix} \begin{pmatrix} \mathbf{e}_0 \\ \mathbf{e}_1 \\ \mathbf{e}_2 \\ \mathbf{e}_3 \end{pmatrix}. \tag{2.15}$$

For Euclidean \mathbf{E}^3 geometry and hyperbolic \mathbf{H}^3 (Bolyai–Lobachevsky) geometry the corresponding π^{ij} matrices ($i, j \in \{0, 1, 2, 3\}$) are respectively:

$$\mathbf{E}^3 : \begin{pmatrix} 0 & 0 & 0 & 0 \\ 0 & 1 & 0 & 0 \\ 0 & 0 & 1 & 0 \\ 0 & 0 & 0 & 1 \end{pmatrix}, \quad \mathbf{H}^3 : \begin{pmatrix} -1 & 0 & 0 & 0 \\ 0 & 1 & 0 & 0 \\ 0 & 0 & 1 & 0 \\ 0 & 0 & 0 & 1 \end{pmatrix}. \tag{2.16}$$

For the other Thurston geometries we include Table 1 from [31], where additional information on the transformation groups are also indicated.

Table 1

The eight Thurston geometries modelled in \mathcal{PS}^3 by a polarity or scalar product and its isometry group.

Space \mathbf{X}	Signature of polarity $\Pi(\star)$ or scalar product $\langle \cdot, \cdot \rangle$ in \mathbf{V}_4	Domain of proper points of \mathbf{X} in \mathcal{PS}^3 ($\mathbf{V}^4(\mathbf{R}), \mathbf{V}_4$)	The group $G = \text{Isom } \mathbf{X}$ as a special collineation group of \mathcal{PS}^3
\mathbf{S}^3	(+ + + +)	\mathcal{PS}^3	Coll \mathcal{PS}^3 preserving $\Pi(\star)$
\mathbf{H}^3	(- + + +)	$\{\mathbf{x} \in \mathcal{P}^3 : \langle \mathbf{x}, \mathbf{x} \rangle < 0\}$	Coll \mathcal{P}^3 preserving $\Pi(\star)$
$\widetilde{\mathbf{SL}_2\mathbf{R}}$	(- - + +) with skew line fibering	Universal covering of $\mathcal{H} := \{[\mathbf{x}] \in \mathcal{PS}^3 : \langle \mathbf{x}, \mathbf{x} \rangle < 0\}$ by fibering transformations	Coll \mathcal{PS}^3 preserving $\Pi(\star)$ and fibres with 4 parameters.
\mathbf{E}^3	(0 + + +)	$\mathcal{A}^3 = \mathcal{P}^3 \setminus \{\omega^\infty\}$ where $\omega^\infty := (\mathbf{b}^0), \mathbf{b}_\star^0 = \mathbf{0}$	Coll \mathcal{P}^3 preserving $\Pi(\star)$, generated by plane reflections
$\mathbf{S}^2 \times \mathbf{R}$	(0 + + +) with O -line bundle fibering	$\mathcal{A}^3 \setminus \{O\}$ O is a fixed origin	G is generated by plane reflections and sphere inversions, leaving invariant the O -concentric 2-spheres of $\Pi(\star)$
$\mathbf{H}^2 \times \mathbf{R}$	(0 - + +) with O -line bundle fibering	$\mathcal{C}^+ = \{X \in \mathcal{A}^3 : \langle \overrightarrow{OX}, \overrightarrow{OX} \rangle < 0, \text{ half cone}\}$ by fibering	G is generated by plane reflections and hyperboloid inversions, leaving invariant the O -concentric half-hyperboloids in the half-cone \mathcal{C}^+ by $\Pi(\star)$
\mathbf{Sol}	(0 - + +) and parallel plane fibering with an ideal plane ϕ	$\mathcal{A}^3 = \mathcal{P}^3 \setminus \phi$	Coll. of \mathcal{A}^3 preserving $\Pi(\star)$ and the fibering with 3 parameters
\mathbf{Nil}	Null-polarity $\Pi(\star)$ with parallel line bundle fibering F with its polar ideal plane ϕ	$\mathcal{A}^3 = \mathcal{P}^3 \setminus \phi$	Coll. of \mathcal{A}^3 preserving $\Pi(\star)$ with 4 parameters

3. $\mathbf{S}^2 \times \mathbf{R}$ and $\mathbf{H}^2 \times \mathbf{R}$ spaces

Of the rich literature not directly related to the projective model of two considered geometries examined, only a few would now be highlighted. In the nice papers [29, 41, 50] the authors investigated the topic of special surfaces of the above geometries, among others, surfaces of constant mean curvature (CMC) surfaces involved minimal surfaces (these surfaces are generally different from constant Gaussian curvature surfaces) (see the further references given in them). In [42] L. Németh studied Pascal pyramids in the $\mathbf{H}^2 \times \mathbf{R}$ space whose examination has led to nice combinatorial and number theoretical correlations.

3.1. Geodesic curves in $\mathbf{S}^2 \times \mathbf{R}$ geometry

In this section we recall important notions and results from the papers [30, 45, 47, 48, 56, 61, 62, 65, 66, 82].

The well-known infinitesimal arc-length square at any point of $\mathbf{S}^2 \times \mathbf{R}$ is the following

$$(ds)^2 = \frac{(dx)^2 + (dy)^2 + (dz)^2}{x^2 + y^2 + z^2}. \tag{3.1}$$

We shall apply the usual geographical coordinates (ϕ, θ) , $(-\pi < \phi \leq \pi, -\frac{\pi}{2} \leq \theta \leq \frac{\pi}{2})$ of the sphere with the fibre coordinate $t \in \mathbf{R}$. We describe points in the above coordinate system in our model by the following equations:

$$x^0 = 1, \quad x^1 = e^t \cos \theta, \quad x^2 = e^t \sin \theta \cos \phi, \quad x^3 = e^t \sin \theta \sin \phi. \tag{3.2}$$

Then we have $x = \frac{x^1}{x^0} = x^1, y = \frac{x^2}{x^0} = x^2, z = \frac{x^3}{x^0} = x^3$, i.e. the usual Cartesian coordinates. By [30] we obtain that in this parametrization the infinitesimal arc-length square at any point of $\mathbf{S}^2 \times \mathbf{R}$ is the following

$$(ds)^2 = (dt)^2 + (d\phi)^2 \cos^2 \theta + (d\theta)^2. \tag{3.3}$$

The geodesic curves of $\mathbf{S}^2 \times \mathbf{R}$ are generally defined as having locally minimal arc length between any two (near enough) points. The system of equations of the parametrized geodesic curves $\gamma(t(\tau), \phi(\tau), \theta(\tau))$ in our model can be determined by the general theory of Riemannian geometry (see [23], [62]).

Then by (3.1-2) we obtain the system of equations of a geodesic curve in our Euclidean model (see [61] and Fig. 1.):

$$\begin{aligned} x(\tau) &= e^{\tau \sin v} \cos(\tau \cos v), \\ y(\tau) &= e^{\tau \sin v} \sin(\tau \cos v) \cos u, \\ z(\tau) &= e^{\tau \sin v} \sin(\tau \cos v) \sin u, \\ -\pi < u &\leq \pi, \quad -\frac{\pi}{2} \leq v \leq \frac{\pi}{2}. \end{aligned} \tag{3.4}$$

3.2. Geodesic curves in $\mathbf{H}^2 \times \mathbf{R}$ geometry

In this section we recall the important notions and results from the papers [30, 47, 63].

The points of $\mathbf{H}^2 \times \mathbf{R}$, form an open cone in projective space \mathcal{P}^3 , as follows:

$$\mathbf{H}^2 \times \mathbf{R} := \{X(\mathbf{x} = x^i \mathbf{e}_i) \in \mathcal{P}^3 : -(x^1)^2 + (x^2)^2 + (x^3)^2 < 0 < x^0, x^1\}.$$

E. Molnár [30] found the infinitesimal arc length square, at any point of $\mathbf{H}^2 \times \mathbf{R}$ as follows

$$\begin{aligned} (ds)^2 &= \frac{1}{(-x^2 + y^2 + z^2)^2} \cdot \left[[(x)^2 + (y)^2 + (z)^2](dx)^2 + \right. \\ &+ 2dxdy(-2xy) + 2dxdz(-2xz) + [(x)^2 + (y)^2 - (z)^2](dy)^2 + \\ &\left. + 2dydz(2yz) + [(x)^2 - (y)^2 + (z)^2](dz)^2 \right]. \end{aligned} \tag{3.5}$$

This simplifies in the cylindrical coordinates (t, r, α) , $(r \geq 0, -\pi < \alpha \leq \pi)$ with fibre coordinate $t \in \mathbf{R}$. Points in our model are then

$$x^0 = 1, \quad x^1 = e^t \cosh r, \quad x^2 = e^t \sinh r \cos \alpha, \quad x^3 = e^t \sinh r \sin \alpha. \tag{3.6}$$

Then we have $x = \frac{x^1}{x^0} = x^1, y = \frac{x^2}{x^0} = x^2, z = \frac{x^3}{x^0} = x^3$, i.e., the usual Cartesian coordinates. We obtain by [30] that in this parametrization the infinitesimal arc-length square in (3.5) at an arbitrary point of $\mathbf{H}^2 \times \mathbf{R}$ is

$$(ds)^2 = (dt)^2 + (dr)^2 + \sinh^2 r (d\alpha)^2. \tag{3.7}$$

The geodesic curves of $\mathbf{H}^2 \times \mathbf{R}$ are generally defined as having locally minimal arc length between any two (near enough) points. The systems of equations of the parametrized geodesic curves $\gamma(t(\tau), r(\tau), \alpha(\tau))$ in our model can be determined by the general theory of Riemannian geometry (see [63]).

Then by (3.6-7) we obtain the system of equations for a geodesic curve in our model (see [63] and Fig. 2.):

$$\begin{aligned} x(\tau) &= e^{\tau \sin v} \cosh(\tau \cos v), \\ y(\tau) &= e^{\tau \sin v} \sinh(\tau \cos v) \cos u, \\ z(\tau) &= e^{\tau \sin v} \sinh(\tau \cos v) \sin u, \\ -\pi < u &\leq \pi, \quad -\frac{\pi}{2} \leq v \leq \frac{\pi}{2}. \end{aligned} \tag{3.8}$$

3.3. Distances and spheres

Let X be one of the two geometries, $X \in \{\mathbf{S}^2 \times \mathbf{R}, \mathbf{H}^2 \times \mathbf{R}\}$. Using geodesic curves, we introduced in [30, 45, 62, 48, 56, 61, 47, 63] the notions of geodesic distance in X .

Definition 3.1. The distance $d^X(P_1, P_2)$ between the points P_1 and P_2 is defined by the arc length of the geodesic curve from P_1 to P_2 .

Definition 3.2. The geodesic sphere of radius ρ (denoted by $S_{P_1}^X(\rho)$) with centre at P_1 is defined as the set of all points P_2 in the space with the condition $d^X(P_1, P_2) = \rho$. Moreover, we require that the geodesic sphere is a simply connected surface without self-intersection in X space (Fig.1, 2).

Definition 3.3. The body of the geodesic sphere with centre P_1 and radius ρ in X space is called geodesic ball, and denoted by $B_{P_1}(\rho)$, i.e., $Q \in B_{P_1}(\rho)$ if and only if $0 \leq d(P_1, Q) \leq \rho$.

Proposition 3.4. A geodesic sphere and ball of radius ρ exists in the $\mathbf{S}^2 \times \mathbf{R}$ space if and only if $\rho \in [0, \pi]$.

Proposition 3.5. $S(\rho)$ is a simply connected surface in $\mathbf{H}^2 \times \mathbf{R}$ for $\rho > 0$.

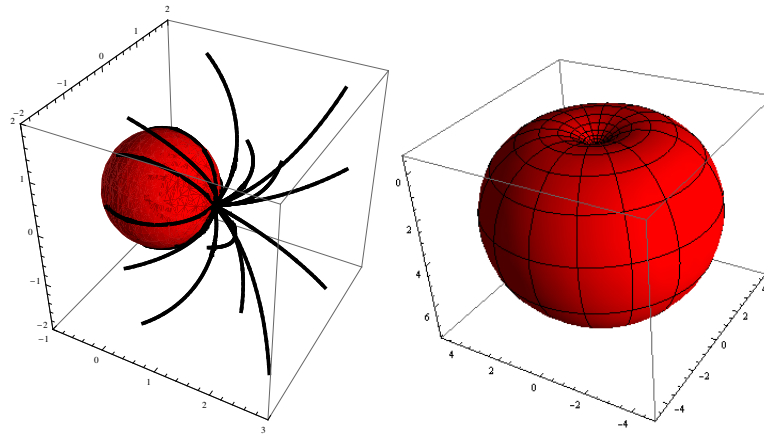


Figure 1. a. Geodesics with varying parameters. b. The geodesic sphere with radius 2 centered at (1, 1, 0, 0).

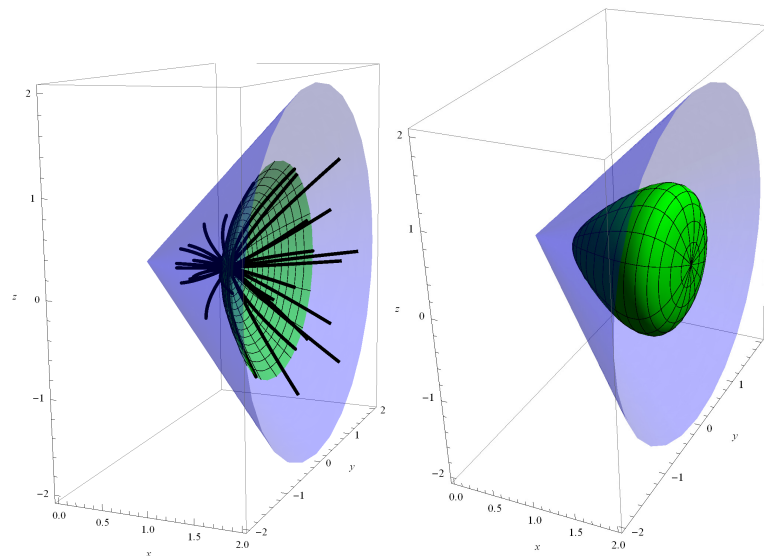


Figure 2. a. Geodesics with varying parameters b. The "base-hyperboloid" in the cone and a geodesic sphere with radius $\frac{2}{3}$ centered at (1, 1, 0, 0) in $\mathbf{H}^2 \times \mathbf{R}$.

3.4. Geodesic triangles and their interior angle sums

We recall the important notions related to the interior angle sums of geodesic triangles in the above geometries elaborated in [65].

A geodesic triangle in Riemannian geometry and more generally in metric geometry is a figure consisting of three different points together with pairwise-connecting geodesic curves. The points are known as the vertices, while the geodesic curve segments are known as the sides of the triangle.

In the geometries of constant curvature $\mathbf{E}^3, \mathbf{H}^3, \mathbf{S}^3$ the well-known sums of the interior angles of geodesic triangles characterize the space. This is related to the Gauss-Bonnet theorem which states that the integral of the Gauss curvature on a compact 2-dimensional Riemannian manifold M is equal to $2\pi\chi(M)$ where $\chi(M)$ denotes the Euler characteristic of M . This theorem has a generalization to any compact even-dimensional Riemannian manifold (see e.g. [5], [23]).

Therefore, it is interesting to investigate the interior angle sums of geodesic triangles in Thurston geometries.

We consider three points A_1, A_2, A_3 in the projective model of the space X (see Section 2) ($X \in \{\mathbf{S}^2 \times \mathbf{R}, \mathbf{H}^2 \times \mathbf{R}\}$). Three geodesic segments a_k connecting the points A_i and A_j ($i < j, i, j, k \in \{1, 2, 3\}, k \neq i, j$) are called sides of the geodesic triangle with vertices A_1, A_2, A_3 (see Fig. 4).

In Riemannian geometry the infinitesimal arc length square (see (3.1) and (3.5)) is used to define the angle θ between two geodesic curves. If their tangent vectors at their common point are \mathbf{u} and \mathbf{v} and g_{ij} are the components of the metric tensor then

$$\cos(\theta) = \frac{u^i g_{ij} v^j}{\sqrt{u^i g_{ij} u^j} \sqrt{v^i g_{ij} v^j}}, \theta \in [0, \pi]. \tag{3.9}$$

Considering a geodesic triangle $A_1 A_2 A_3$ we can assume by the homogeneity of the geometries considered that one vertex coincides with the point $A_1 = (1, 1, 0, 0)$ and the other two vertices are $A_2 = (1, x_2, y_2, z_2)$ and $A_3 = (1, x_3, y_3, z_3)$.

We investigated the interior angles and their sums of geodesic triangles in $\mathbf{S}^2 \times \mathbf{R}$ and $\mathbf{H}^2 \times \mathbf{R}$ geometries (see [65]).

The answer to the question about the sum of angles of a geodesic triangle is a direct consequence of the comparison theorems in Riemannian geometry (Toponogov and Alexandrov's theorems, see [6]), since the sectional curvature of $\mathbf{S}^2 \times \mathbf{R}$ is non-negative and the sectional curvature of $\mathbf{H}^2 \times \mathbf{R}$ is non-positive.

3.4.1. Interior angle sums in $\mathbf{S}^2 \times \mathbf{R}$ geometry We gave a new direct approach to this question based on the projective model and the isometry groups of $\mathbf{S}^2 \times \mathbf{R}$ and $\mathbf{H}^2 \times \mathbf{R}$ in [65].

We directly obtained from equations (3.4) of geodesic curves the following

Lemma 3.6 ([65]). *Let P be an arbitrary point and $g(A_1, P)$ ($A_1 = (1, 1, 0, 0)$) be a geodesic curve in the projective model of the $\mathbf{S}^2 \times \mathbf{R}$ geometry. The points of the geodesic curve $g(A_1, P)$ and the centre of the model E_0 lie in a plane in the Euclidean sense (see Fig. 3).*

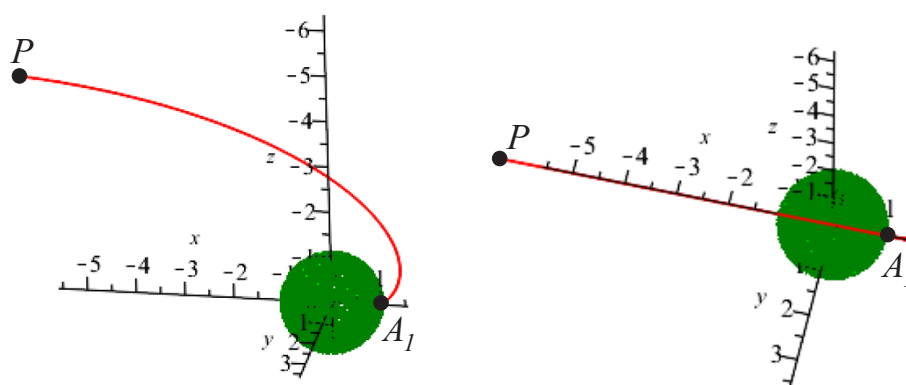


Figure 3. Geodesic curve $g(A_1, P)$ ($A_1 = (1, 1, 0, 0)$) and $P \in \mathbf{S}^2 \times \mathbf{R}$ with "base plane", the plane of the geodesic curve contains the origin $E_0 = (1, 0, 0, 0)$ of the model [65].

Theorem 3.7 ([65]). *If the Euclidean plane of the vertices of an $\mathbf{S}^2 \times \mathbf{R}$ geodesic triangle $A_1 A_2 A_3$ contains the centre of model E_0 then its interior angle sum is equal to π .*

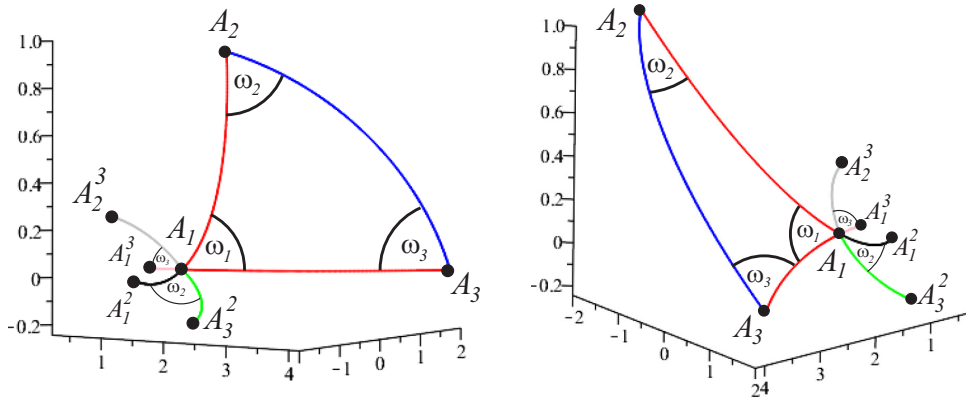


Figure 4. A geodesic triangle with vertices $A_1 = (1, 1, 0, 0)$, $A_2 = (1, 3, -2, 1)$, $A_3 = (1, 2, 1, 0)$ in $S^2 \times \mathbf{R}$ geometry, and the transformed images of its geodesic side segments [65].

We could determine the interior angle sum of arbitrary geodesic triangle (for some numerical results see [65]).

We obtained the following

Theorem 3.8 ([65]). *If the Euclidean plane of the vertices of an $S^2 \times \mathbf{R}$ geodesic triangle $A_1A_2A_3$ does not contain the centre of the model E_0 then its interior angle sum is greater than π .*

Remark 3.9. *It is well known that if the vertices A_1, A_2, A_3 lie on a sphere of radius $R \in \mathbf{R}^+$ centred at E_0 then the interior angle sum of the spherical triangle $A_1A_2A_3$ is greater than π .*

In summary we have the following

Theorem 3.10 ([65]). *The sum of the interior angles of a geodesic triangle of $S^2 \times \mathbf{R}$ is greater than or equal to π .*

3.4.2. *Interior angle sums in $H^2 \times \mathbf{R}$ geometry* Similarly to the $S^2 \times \mathbf{R}$ space we investigated the interior angles of a geodesic triangle $A_1A_2A_3$ and its interior angle sum $\sum_{i=1}^3(\omega_i)$ in the $H^2 \times \mathbf{R}$ space (see [65] and Fig. 6).

Lemma 3.11 ([65]). *Let P be an arbitrary point and $g(A_1, P)$ ($A_1 = (1, 1, 0, 0)$) be a geodesic curve in the projective model of $H^2 \times \mathbf{R}$ geometry. The points of the geodesic curve $g(A_1, P)$ and the centre of the model E_0 lie in a plane in the Euclidean sense (see Fig. 5).*

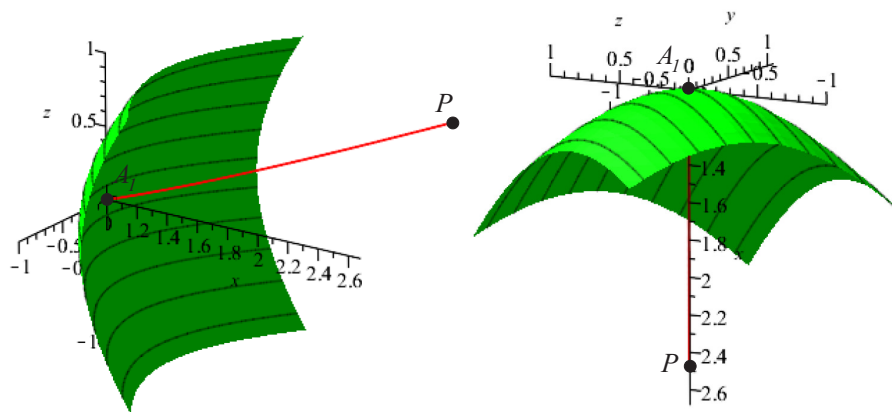


Figure 5. Geodesic curve $g(A_1, P)$ ($A_1 = (1, 1, 0, 0)$ and $P \in H^2 \times \mathbf{R}$) with "base plane" (the "upper" sheet of the two-sheeted hyperboloid), the plane of a geodesic curve contains the origin $E_0 = (1, 0, 0, 0)$ of the model [65].

Remark 3.12. *More information about the isometry group of $H^2 \times \mathbf{R}$ and about its discrete subgroups can be found in [63].*

Theorem 3.13 ([65]). *If the Euclidean plane of the vertices of a $H^2 \times \mathbf{R}$ geodesic triangle $A_1A_2A_3$ contains the centre of the model E_0 then its interior angle sum is equal to π .*

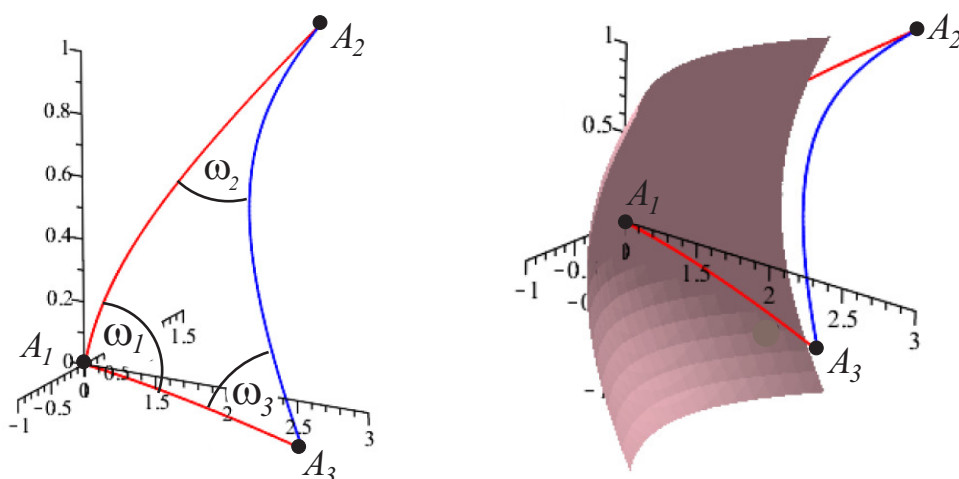


Figure 6. Geodesic triangle with vertices $A_1 = (1, 1, 0, 0)$, $A_2 = (1, 2, 3/2, 1)$, $A_3 = (1, 3, -1, 0)$ in $\mathbf{H}^2 \times \mathbf{R}$ geometry [65].

We can determine the interior angle sum of an arbitrary $\mathbf{H}^2 \times \mathbf{R}$ geodesic triangle.

We have the following

Theorem 3.14 ([65]). *If the Euclidean plane of the vertices of a $\mathbf{H}^2 \times \mathbf{R}$ geodesic triangle $A_1 A_2 A_3$ does not contain the centre of model E_0 then its interior angle sum is less than π .*

Remark 3.15. *It is well known that if the vertices A_1, A_2, A_3 lie on an "upper" sheet of the two-sheeted hyperboloid (in the hyperboloid model of the hyperbolic plane geometry where the straight lines of hyperbolic 2-space are modelled by geodesics on the hyperboloid) centred at E_0 then the interior angle sum of hyperbolic triangle $A_1 A_2 A_3$ is less than π .*

In summary we obtained the following

Theorem 3.16 ([65]). *The sum of the interior angles of a geodesic triangle of $\mathbf{H}^2 \times \mathbf{R}$ space is less than or equal to π .*

3.5. Surfaces of geodesic triangles

We consider 3 points A_0, A_1, A_2 in the projective model of the X space (see Section 2, subsections 3.1-2) ($X \in \{\mathbf{S}^2 \times \mathbf{R}, \mathbf{H}^2 \times \mathbf{R}\}$). The geodesic segments a_k connecting the points A_i and A_j ($i < j, i, j, k \in \{0, 1, 2\}, k \neq i, j$) are called sides of the geodesic triangle with vertices A_0, A_1, A_2 .

The definition of the surface of a geodesic triangle in the space X is not straightforward. The usual geodesic triangle surface's definition in these geometries is not possible because the geodesic curves starting from different vertices and ending at points of the corresponding opposite edges define different surfaces, i.e. geodesics starting from different vertices and ending at points on the corresponding opposite side usually do not intersect. Therefore, we introduced the definition (see [66]) of the surface $\mathcal{S}_{A_0 A_1 A_2}$ of the geodesic triangle using the notion of the generalized Apollonius surfaces:

Definition 3.17. The Apollonius surface $\mathcal{AS}_{P_1 P_2}^X(\lambda)$ in the Thurston geometry X is the set of all points of X whose geodesic distances from two fixed points are in a constant ratio $\lambda \in \mathbf{R}_0^+$ where $X \in \mathbf{E}^3, \mathbf{S}^3, \mathbf{H}^3, \mathbf{S}^2 \times \mathbf{R}, \mathbf{H}^2 \times \mathbf{R}, \mathbf{Nil}, \widetilde{\mathbf{SL}}_2 \mathbf{R}, \mathbf{Sol}$. i.e. $\mathcal{AS}_{P_1 P_2}^X(\lambda)$ of two arbitrary points $P_1, P_2 \in X$ consists of all points $P' \in X$, for which $d^X(P_1, P') = \lambda \cdot d^X(P', P_2)$ ($\lambda \in [0, \infty)$) where d^X is the corresponding distance function of X . If $\lambda = 0$, then $\mathcal{AS}_{P_1 P_2}^X(0) := P_1$ and it is clear, that in case $\lambda \rightarrow \infty$ then $d^X(P', P_2) \rightarrow 0$ therefore we say $\mathcal{AS}_{P_1 P_2}^X(\infty) := P_2$.

We consider the geodesic triangle $A_0 A_1 A_2$ in the projective model of X space ($X \in \{\mathbf{S}^2 \times \mathbf{R}, \mathbf{H}^2 \times \mathbf{R}\}$) and consider the Apollonius surfaces $\mathcal{AS}_{A_0 A_1}^X(\lambda_1)$ and $\mathcal{AS}_{A_2 A_0}^X(\lambda_2)$ ($\lambda_1, \lambda_2 \in [0, \infty), \lambda_1^2 + \lambda_2^2 > 0$). It is clear, that if $Y \in \mathcal{C}(\lambda_1, \lambda_2) := \mathcal{AS}_{A_0 A_1}^X(\lambda_1) \cap \mathcal{AS}_{A_2 A_0}^X(\lambda_2)$ then $\frac{d^X(A_0, Y)}{d^X(Y, A_1)} = \lambda_1$ and $\frac{d^X(A_2, Y)}{d^X(Y, A_0)} = \lambda_2 \Rightarrow \frac{d^X(A_2, Y)}{d^X(Y, A_1)} = \lambda_1 \cdot \lambda_2$ for parameters $\lambda_1, \lambda_2 \in (0, \infty)$ and if $\lambda_1 = 0$ then $\mathcal{C}(\lambda_1, \lambda_2) = A_0$, if $\lambda_2 = 0$ then $\mathcal{C}(\lambda_1, \lambda_2) = A_2$

Definition 3.18. 1.

$$P^X(\lambda_1, \lambda_2) := \{P \in X \mid P \in \mathcal{C}(\lambda_1, \lambda_2) \text{ and } d^X(P, A_0) = \min_{Q \in \mathcal{C}(\lambda_1, \lambda_2)} (d^X(Q, A_0))\} \tag{3.10}$$

with given real parameters $\lambda_1, \lambda_2 \in [0, \infty), \lambda_1^2 + \lambda_2^2 > 0$

2. The surface $S_{A_0A_1A_2}^X$ of the geodesic triangle $A_0A_1A_2$ is

$$S_{A_0A_1A_2}^X := \{P^X(\lambda_1, \lambda_2) \in X, \text{ where } \lambda_1, \lambda_2 \in [0, \infty), \lambda_1^2 + \lambda_2^2 > 0\}. \quad (3.11)$$

We obtained the following implicit equation of the Apollonius surfaces $AS_{P_1P_2}^X(\lambda)$ of two proper points $P_1(1, a, b, c)$ and $P_2(1, d, e, f)$ with given ratio $\lambda \in \mathbf{R}_0^+$, in X geometry:

Theorem 3.19 ([66]). *The implicit equation of the Apollonius surfaces $AS_{P_1P_2}^X(\lambda)$ of two proper points $P_1(1, a, b, c)$ and $P_2(1, d, e, f)$ with given ratio $\lambda \in \mathbf{R}_0^+$, in the X geometry is:*

$$\begin{aligned} AS_{P_1P_2}^X(\lambda)(x, y, z) \Rightarrow \\ 4\omega_X^2 \left(\frac{ax \pm by \pm cz}{\sqrt{a^2 \pm b^2 \pm c^2} \sqrt{x^2 \pm y^2 \pm z^2}} \right) + \log^2 \left(\frac{a^2 \pm b^2 \pm c^2}{x^2 \pm y^2 \pm z^2} \right) = \\ = \lambda^2 \left[4\omega_X^2 \left(\frac{dx \pm ey \pm fz}{\sqrt{d^2 \pm e^2 \pm f^2} \sqrt{x^2 \pm y^2 \pm z^2}} \right) + \log^2 \left(\frac{d^2 \pm e^2 \pm f^2}{x^2 \pm y^2 \pm z^2} \right) \right], \end{aligned}$$

where if $X = \mathbf{S}^2 \times \mathbf{R}$ then all \pm signs are $+$, $\omega_X(x) = \arccos(x)$ and if $X = \mathbf{H}^2 \times \mathbf{R}$ then the all \pm signs are $-$, $\omega_X(x) = \operatorname{arccosh}(x)$ (see Fig. 7, 8).

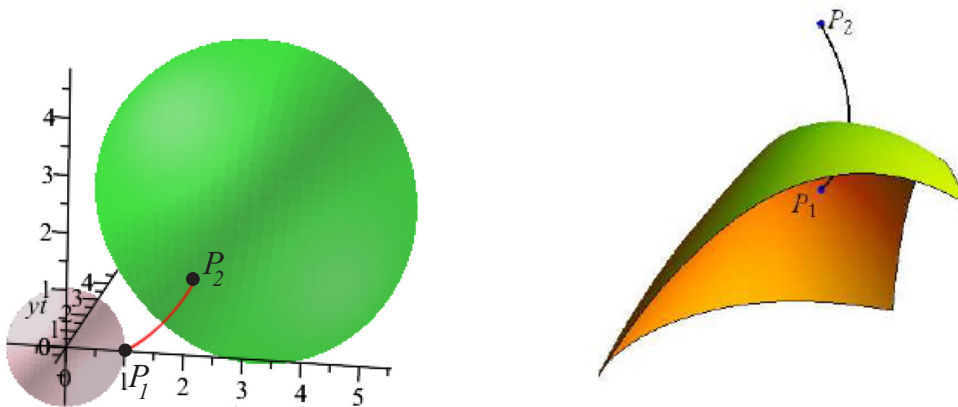


Figure 7. The Apollonius surface $AS_{P_1P_2}^{\mathbf{S}^2 \times \mathbf{R}}(\lambda)$ where $P_1 = (1, 1, 0, 0)$, $P_2 = (1, 2, 1, 1)$, $\lambda = 2$ (left) and $\lambda = 1$ (right, equidistance surface (see [66, 45])

We used the statement of the following lemma

Lemma 3.20 ([65]). *Let P be an arbitrary point, $g^X(P_1, P)$ ($X \in \{\mathbf{S}^2 \times \mathbf{R}, \mathbf{H}^2 \times \mathbf{R}\}$, and $P_1 = (1, 1, 0, 0)$) a geodesic curve in the considered model of X geometry. The points of the geodesic curve $g^X(P_1, P)$ and the centre of the model $E_0 = (1, 0, 0, 0)$ lie in a Euclidean plane.*

3.6. Geodesic tetrahedra and their circumscribed spheres

We consider 4 points A_0, A_1, A_2, A_3 in the projective model of the space X (see Section 2, subsections 3.1-2 $X \in \{\mathbf{S}^2 \times \mathbf{R}, \mathbf{H}^2 \times \mathbf{R}\}$). These points are the vertices of a *geodesic tetrahedron* in the space X if any two *geodesic segments* connecting the points A_i and A_j ($i < j$, $i, j \in \{0, 1, 2, 3\}$) do not have common inner points and any three vertices do not lie on the same geodesic curve. The geodesic segments A_iA_j are called *edges* of the geodesic tetrahedron $A_0A_1A_2A_3$. A circumscribed sphere of a geodesic tetrahedron is a geodesic sphere that touches each of the tetrahedron's vertices. As in the Euclidean case the radius of a geodesic sphere circumscribed around a tetrahedron T is called the *circumradius* of T , and the centre point of this sphere is called the *circumcenter* of T (Fig. 9, 10). For any $\mathbf{S}^2 \times \mathbf{R}$ geodesic tetrahedron there exists a unique geodesic surface on which all four vertices lie. If its radius is less than or equal to π then the above surface is a geodesic sphere called *circumscribed sphere*, (see Definition 3.2 of sphere and [66]).

Remark 3.21. *If the common point of bisectors related to the vertices of a geodesic tetrahedron lies at infinity then the vertices of a geodesic tetrahedron lie on a horosphere-like surface and if the common point is an outer point then the vertices of the tetrahedron are on a hypersphere-like surface. These surfaces will be examined in detail in a forthcoming paper.*

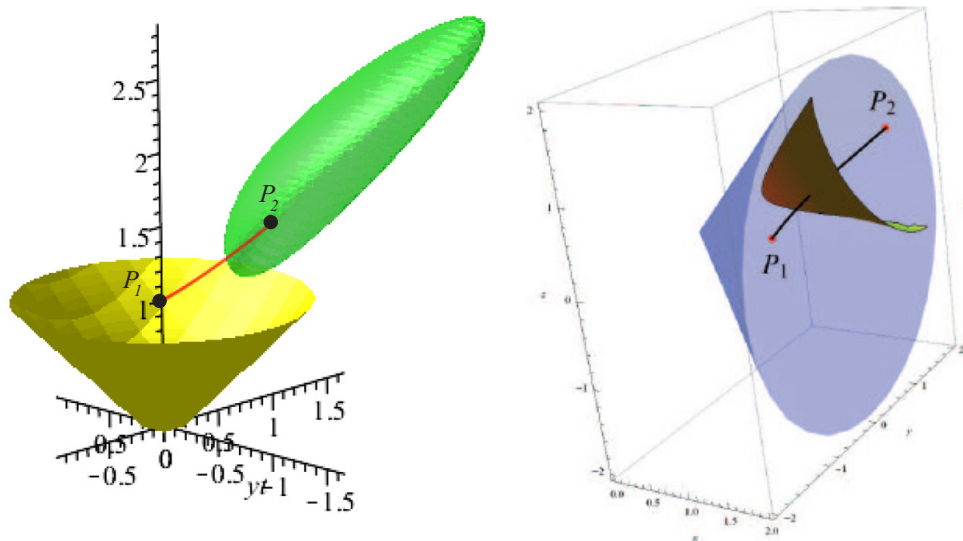


Figure 8. The Apollonius surface $\mathcal{AS}_{P_1 P_2}^{\mathbf{H}^2 \times \mathbf{R}}(\lambda)$ where $P_1 = (1, 1, 0, 0)$, $P_2 = (1, 3/2, 1, -1/2)$, $\lambda = 2$ (left) and $P_1 = (1, 1, 0, 0)$, $P_2 = (1, 2, 1, 1)$, $\lambda = 1$ (right, equidistance surface) (see [66, 47])

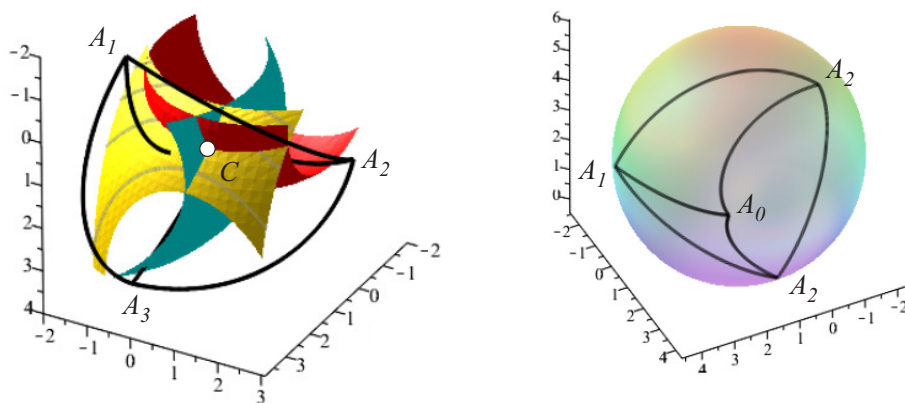


Figure 9. Geodesic $\mathbf{S}^2 \times \mathbf{R}$ tetrahedron with vertices $A_0 = (1, 1, 0, 0)$, $A_1 = (1, -2, -1/2, 3)$, $A_2 = (1, 1, 3, 0)$, $A_3 = (1, 4, -1, 2)$ and its circumscribed sphere of radius $r \approx 1.30678$ with circumcenter $C = (1, \approx 0.64697, \approx 0.51402, \approx 0.15171)$ [66].

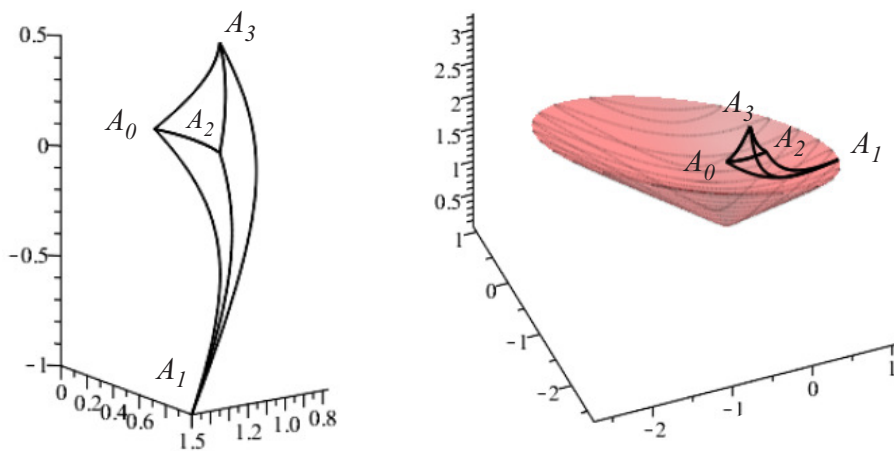
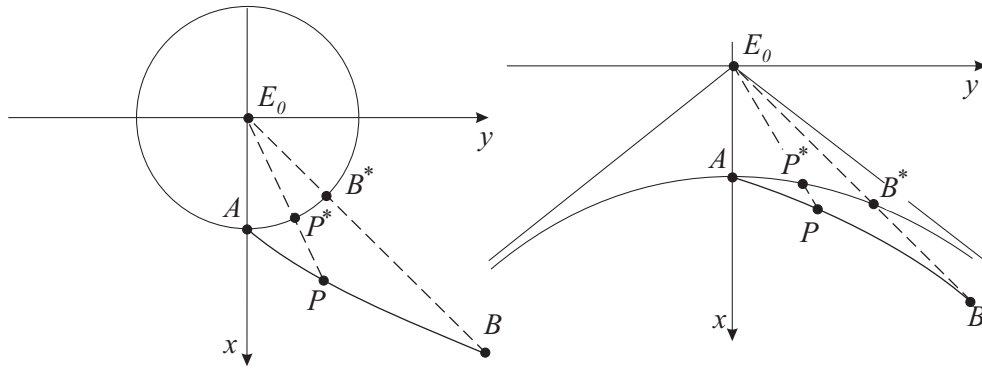


Figure 10. Geodesic $\mathbf{H}^2 \times \mathbf{R}$ tetrahedron with vertices $A_0 = (1, 1, 0, 0)$, $A_1 = (1, 3/2, 1, -1)$, $A_2 = (1, 1, 1/2, 0)$, $A_3 = (1, 1, 1/2, 1/2)$ and its circumscribed sphere of radius $r \approx 2.89269$ with circumcenter $C = (1, \approx 0.07017, \approx -0.02714, \approx -0.02640)$ [66]


 Figure 11. Simple ratios in $S^2 \times \mathbf{R}$ and $\mathbf{H}^2 \times \mathbf{R}$ spaces

For any $\mathbf{H}^2 \times \mathbf{R}$ geodesic tetrahedron there exists a unique geodesic surface on which all four vertices lie. If its centre is a proper point of $\mathbf{H}^2 \times \mathbf{R}$ then the above surface is a geodesic sphere (called a circumscribed sphere) (see Definition 3.2 of sphere and [66]).

3.7. Menelaus' and Ceva's theorems in $S^2 \times \mathbf{R}$ and $\mathbf{H}^2 \times \mathbf{R}$ spaces

First we recall the definition of simple ratios in the sphere S^2 and the plane \mathbf{H}^2 (see [49]). The models of the above plane geometries of constant curvature are embedded in the models of the previously described geometries $S^2 \times \mathbf{R}$ and $\mathbf{H}^2 \times \mathbf{R}$ as "base planes" and are used hereinafter for our discussions.

A spherical triangle is the space enclosed by arcs of great circles on the surface of a sphere, subject to the constraint that these arcs and the further circular arcs in the spherical plane are always less than or equal to a semicircle.

Definition 3.22. If A , B and P are distinct points on a line in $Y \in \{\mathbf{H}^2, S^2\}$, then their simple ratio is $s^Y(A, P, B) = w^Y(d^Y(A, P))/w^Y(d^Y(P, B))$ if P is between A and B , and $s^Y(A, P, B) = -w^Y(d^Y(A, P))/w^Y(d^Y(P, B))$, otherwise where $w^Y(x) := \sin(x)$ if $Y = S^2$ and $w^Y(x) := \sinh(x)$ if $Y = \mathbf{H}^2$.

Remark 3.23. Basic properties of simple ratio:

1. $s^Y(A, P, B) = 1/s^Y(B, P, A)$,
2. if P is between A and B , then $s^Y(A, P, B) \in (0, \infty)$,
3. if P is on AB , beyond B , then $s^Y(A, P, B) \in (-\infty, -1)$,
4. if P is on AB , beyond A , then $s^Y(A, P, B) \in (-1, 0)$.

Note that the value of $s^Y(A, P, B)$ determines the position of P relative to A and B .

With this definition, the corresponding sine rule of the geometry Y leads to Menelaus' and Ceva's theorems [28, 49]:

Theorem 3.24 (Menelaus' Theorem for triangles in the plane Y). If a line l not passing through any vertex of a triangle ABC is such that l meets BC in Q , AC in R , and AB in P , then

$$s^Y(A, P, B)s^Y(B, Q, C)s^Y(C, R, A) = -1.$$

Theorem 3.25 (Ceva's Theorem for triangles in the plane Y). If T is a point not on any side of a triangle ABC such that AT and BC meet in Q , BT and AC in R , and CT and AB in P , then

$$s^Y(A, P, B)s^Y(B, Q, C)s^Y(C, R, A) = 1.$$

3.8. Generalizations of Menelaus' and Ceva's theorems

3.8.1. Geodesic triangle in general position First we consider a general location geodesic triangle $A_0A_1A_2$ in the projective model of the space X (see subsections 3.1-2) ($X \in \{S^2 \times \mathbf{R}, \mathbf{H}^2 \times \mathbf{R}\}$). Without loss of generality, we can assume that $A_0 = (1, 1, 0, 0)$ and A_2 lies in the coordinate plane $[x, y]$. The geodesic lines that contain the

sides A_0A_1 and A_0A_2 of the given triangle can be characterized directly by the corresponding parameters v and u (see (3.4) and (3.8)).

The geodesic curve including the side segment A_1A_2 is also determined by one of its endpoints and its parameters, however in order to determine the corresponding parameters of this geodesic line we use *orientation preserving isometric transformations* $\mathbf{T}^X(A_2)$, as elements of the isometry group of the geometry X , that maps $A_2 = (1, x_2, y_2, 0)$ onto $A_0 = (1, 1, 0, 0)$ (up to a positive determinant factor).

We extend the definition of the simple ratio to the $X \in \{\mathbf{S}^2 \times \mathbf{R}, \mathbf{H}^2 \times \mathbf{R}\}$ spaces. If $X = \mathbf{S}^2 \times \mathbf{R}$ then it is clear that the space contains its "base sphere" (unit sphere centred in E_0) which is a geodesic surface. Therefore, similarly to the spherical spaces we assume that the geodesic arcs are always less than or equal to a semicircle (at present π).

Definition 3.26. If A, B and P are distinct points on a non-fiber-like geodesic curve in the $X \in \{\mathbf{S}^2 \times \mathbf{R}, \mathbf{H}^2 \times \mathbf{R}\}$ space, then their simple ratio is

$$s_g^X(A, P, B) = w^X(d^X(A, P)\cos(v)) / w^X(d^X(P, B)\cos(v)),$$

if P is between A and B , and

$$s_g^X(A, P, B) = -w^X(d^X(A, P)\cos(v)) / w^X(d^X(P, B)\cos(v)),$$

where $w^X(x) := \sin(x)$ if $X = \mathbf{S}^2 \times \mathbf{R}$, $w^X(x) := \sinh(x)$ if $X = \mathbf{H}^2 \times \mathbf{R}$ and v is the parameter of the geodesic curve containing points A, B and P (see Fig. 11).

Theorem 3.27 (Ceva's Theorem for triangles in general location, [66]). *If T is a point not contained in any side of a geodesic triangle $A_0A_1A_2$ in $X \in \{\mathbf{S}^2 \times \mathbf{R}, \mathbf{H}^2 \times \mathbf{R}\}$ such that the curves A_0T and $g_{A_1A_2}^X$ meet in Q , A_1T and $g_{A_0A_2}^X$ in R , and A_2T and $g_{A_0A_1}^X$ in P , ($A_0T, A_1T, A_2T \subset \mathcal{S}_{A_0A_1A_2}^X$) then*

$$s_g^X(A_0, P, A_1)s_g^X(A_1, Q, A_2)s_g^X(A_2, R, A_0) = 1.$$

Theorem 3.28 (Menelaus's theorem for triangles in general location, [66]). *If l is a line not through any vertex of a geodesic triangle $A_0A_1A_2$ lying in a surface $\mathcal{S}_{A_0A_1A_2}^X$ in the $X \in \{\mathbf{S}^2 \times \mathbf{R}, \mathbf{H}^2 \times \mathbf{R}\}$ geometry such that l meets the geodesic curves $g_{A_1A_2}^X$ in Q , $g_{A_0A_2}^X$ in R , and $g_{A_0A_1}^X$ in P , then*

$$s_g^X(A_0, P, A_1)s_g^X(A_1, Q, A_2)s_g^X(A_2, R, A_0) = -1.$$

3.8.2. Fibre type triangle We consider a *fibre type geodesic triangle* $A_0A_1A_2$ in the projective model of the space X . Without limiting generality, we can assume that $A_0 = (1, 1, 0, 0)$, $A_1 = (1, x_1, y_1, 0)$ and $A_2 = (1, x_2, y_2, 0)$ lie in the coordinate plane $[x, y]$. The geodesic lines that contain the sides A_0A_1 and A_0A_2 of the given triangle can be characterized directly by the corresponding parameters v and $u = 0$ similar to the above case.

We extend the definition of the simple ratio to the $X \in \{\mathbf{S}^2 \times \mathbf{R}, \mathbf{H}^2 \times \mathbf{R}\}$ spaces.

If $X = \mathbf{S}^2 \times \mathbf{R}$ it is clear that the $\mathbf{S}^2 \times \mathbf{R}$ space contains its "base sphere" (unit sphere centred in E_0) which is a geodesic surface. Therefore, similarly to the spherical spaces we assume that the geodesic arcs are always less than or equal to a semicircle (at present π).

Definition 3.29. If A, B and P are distinct points on fibrum-like geodesic curve in the $X \in \{\mathbf{S}^2 \times \mathbf{R}, \mathbf{H}^2 \times \mathbf{R}\}$ space, then their simple ratio is

$$s_f^X(A, P, B) = d^X(A, P) / d^X(P, B)$$

if P is between A and B , and

$$s_f^X(A, P, B) = -d^X(A, P) / d^X(P, B)$$

(see Fig. 11).

Theorem 3.30 (Ceva's Theorem in the X geometry for triangles in fibre types, [66]). *If T is a point not on any side of a geodesic triangle $A_0A_1A_2$ in $X \in \{\mathbf{S}^2 \times \mathbf{R}, \mathbf{H}^2 \times \mathbf{R}\}$ such that the geodesic curves $g_{A_0T}^X$ and $g_{A_1A_2}^X$ meet in Q , $g_{A_1T}^X$ and $g_{A_0A_2}^X$ in R , and $g_{A_2T}^X$ and $g_{A_0A_1}^X$ in P , ($g_{A_0T}^X, g_{A_1T}^X, g_{A_2T}^X \subset \mathcal{S}_{A_0A_1A_2}^X$) then*

$$s_f^X(A_0, P, A_1)s_f^X(A_1, Q, A_2)s_f^X(A_2, R, A_0) = 1.$$

Theorem 3.31 (Menelaus’s theorem in the X geometry for triangles in fibre types, [66]). *If l is a line not through any vertex of a geodesic triangle $A_0A_1A_2$ lying in its surface $S_{A_0A_1A_2}^X$ in $X \in \{\mathbf{S}^2 \times \mathbf{R}, \mathbf{H}^2 \times \mathbf{R}\}$ geometry such that l meets the geodesic curves $g_{A_1A_2}^X$ in Q , $g_{A_0A_2}^X$ in R , and $g_{A_0A_1}^X$ in P , then*

$$s_f^X(A_0, P, A_1)s_f^X(A_1, Q, A_2)s_f^X(A_2, R, A_0) = -1.$$

Thus, we can formulate similar theorems for the fibre-like geodesic triangle as for the corresponding Euclidean triangles; therefore the Ceva’s and Menelaus’ theorems in the geometry X follow from the well-known corresponding Euclidean cases.

4. Nil space

In her dissertation [3] K. Brodaczewska studied some aspects of the elementary geometry and in [43] the authors discussed the visualization of the Nil geometry. In the papers [34, 46, 52, 51] we investigated the equidistant surfaces, parallelohedra, crystallography, and another possible model (so called linear model) of Nil geometry. In [22] J. Inoguchi classified the minimal translation surfaces of the considered space.

In this Section we summarize the relevant notions and notation (see [30], [55]).

4.1. Basic notions of Nil geometry

Nil geometry is a homogeneous 3-space derived from the famous real matrix group $\mathbf{L}(\mathbf{R})$, used by W. Heisenberg in his electro-magnetic studies. The Lie theory with the method of projective geometry makes possible to describe this topic.

The left (row-column) multiplication of Heisenberg matrices

$$\begin{pmatrix} 1 & x & z \\ 0 & 1 & y \\ 0 & 0 & 1 \end{pmatrix} \begin{pmatrix} 1 & a & c \\ 0 & 1 & b \\ 0 & 0 & 1 \end{pmatrix} = \begin{pmatrix} 1 & a+x & c+xb+z \\ 0 & 1 & b+y \\ 0 & 0 & 1 \end{pmatrix} \tag{4.1}$$

defines the “translations” $\mathbf{L}(\mathbf{R}) = \{(x, y, z) : x, y, z \in \mathbf{R}\}$ on the points of $\text{Nil} = \{(a, b, c) : a, b, c \in \mathbf{R}\}$. These translations are not commutative, in general. The matrices $\mathbf{K}(z) \triangleleft \mathbf{L}(\mathbf{R})$ of the form

$$\mathbf{K}(z) \ni \begin{pmatrix} 1 & 0 & z \\ 0 & 1 & 0 \\ 0 & 0 & 1 \end{pmatrix} \mapsto (0, 0, z) \tag{4.2}$$

constitute the one parametric centre, i.e., each of its elements commutes with all elements of $\mathbf{L}(\mathbf{R})$. The elements of $\mathbf{K}(z)$ are called *fibre translations*. Nil geometry of the Heisenberg group can be projectively (affinely) interpreted by the “right translations” (see ([30, 31]) on points as the matrix formula

$$(1; a, b, c) \rightarrow (1; a, b, c) \begin{pmatrix} 1 & x & y & z \\ 0 & 1 & 0 & 0 \\ 0 & 0 & 1 & x \\ 0 & 0 & 0 & 1 \end{pmatrix} = (1; x+a, y+b, z+bx+c) \tag{4.3}$$

shows, according to (4.1). Here we consider $\mathbf{L}(\mathbf{R})$ the projective collineation group with right actions in homogeneous coordinates.

E. Molnár [30] derived the well-known infinitesimal arc length square, invariant under translations \mathbf{L} at any point of Nil as follows

$$\begin{aligned} (ds)^2 &:= (dx)^2 + (dy)^2 + (-xdy + dz)^2 = \\ & (dx)^2 + (1+x^2)(dy)^2 - 2x(dy)(dz) + (dz)^2 \end{aligned} \tag{4.4}$$

Hence we obtain the symmetric metric tensor field g on Nil with components g_{ij} , and its inverse:

$$g_{ij} := \begin{pmatrix} 1 & 0 & 0 \\ 0 & 1+x^2 & -x \\ 0 & -x & 1 \end{pmatrix}, \quad g^{ij} := \begin{pmatrix} 1 & 0 & 0 \\ 0 & 1 & x \\ 0 & x & 1+x^2 \end{pmatrix} \tag{4.5}$$

where $\det(g_{ij}) = 1$.

The translation group \mathbf{L} defined by formula (4.3) can be extended to a larger group \mathbf{G} of collineation, preserving the fibering, that will be equivalent to the (orientation preserving) isometry group of \mathbf{Nil} . In [33] E. Molnár has shown that a rotation by angle ω about the z -axis at the origin, as isometry of \mathbf{Nil} , leaves invariant the Riemann metric everywhere, and is a quadratic mapping in x, y to z -image \bar{z} as follows:

$$\begin{aligned} \mathbf{r}(O, \omega) : (1; x, y, z) &\rightarrow (1; \bar{x}, \bar{y}, \bar{z}); \\ \bar{x} &= x \cos \omega - y \sin \omega, \quad \bar{y} = x \sin \omega + y \cos \omega, \\ \bar{z} &= z - \frac{1}{2}xy + \frac{1}{4}(x^2 - y^2) \sin 2\omega + \frac{1}{2}xy \cos 2\omega. \end{aligned} \tag{4.6}$$

This rotation formula, however, is conjugate by the quadratic mapping

$$\begin{aligned} \mathcal{M} : x \rightarrow x' = x, \quad y \rightarrow y' = y, \quad z \rightarrow z' = z - \frac{1}{2}xy \text{ to} \\ (1; x', y', z') \rightarrow (1; x', y', z') \begin{pmatrix} 1 & 0 & 0 & 0 \\ 0 & \cos \omega & \sin \omega & 0 \\ 0 & -\sin \omega & \cos \omega & 0 \\ 0 & 0 & 0 & 1 \end{pmatrix} = (1; x^*, y^*, z^*), \\ \text{with } x^* \rightarrow \bar{x} = x^*, \quad y^* \rightarrow \bar{y} = y^*, \quad z^* \rightarrow \bar{z} = z^* + \frac{1}{2}x^*y^*, \end{aligned} \tag{4.7}$$

i.e., to the linear rotation formula. This quadratic conjugacy modifies the \mathbf{Nil} translations in (4.3), as well. This is characterized by the following important classification theorem.

Theorem 4.1 ([33]). 1. Any group of \mathbf{Nil} isometries, containing a 3-dimensional translation lattice, is conjugate by the quadratic mapping in (4.7) to an affine group of the affine (or Euclidean) space $\mathbf{A}^3 = \mathbf{E}^3$ whose projection onto the (x, y) -plane is an isometry group of \mathbf{E}^2 . Such an affine group preserves a plane \rightarrow point null-polarity.

2. The involutive line reflection about the y axis

$$(1; x, y, z) \rightarrow (1; -x, y, -z),$$

preserves the Riemann metric, and its conjugates by the above isometries in 1 (those of the identity component) are also \mathbf{Nil} -isometries. Orientation reversing \mathbf{Nil} -isometries do not exist.

Remark 4.2. We obtain a new projective model for \mathbf{Nil} geometry from the projective model, derived from the quadratic mapping \mathcal{M} . This is the linearized model of \mathbf{Nil} space (see [3], [33]) that seems to be more advantageous for future study. But we will continue to use the classical Heisenberg model in this survey.

4.2. Geodesic curves, spheres and their properties

The geodesic curves of the \mathbf{Nil} geometry are generally defined as having locally minimal arc length between any two (near enough) points. The system of equations of the parametrized geodesic curves $g(x(t), y(t), z(t))$ in our model can be determined by the Levy–Civita theory of Riemannian geometry. We can assume that the starting point of a geodesic curve is the origin because we can transform a curve to have arbitrary starting point by translation;

$$\begin{aligned} x(0) = y(0) = z(0) = 0; \quad \dot{x}(0) = c \cos \alpha, \quad \dot{y}(0) = c \sin \alpha, \\ \dot{z}(0) = w; \quad -\pi \leq \alpha \leq \pi. \end{aligned}$$

The arc length parameter s is introduced by

$$s = \sqrt{c^2 + w^2} \cdot t, \text{ where } w = \sin \theta, \quad c = \cos \theta, \quad -\frac{\pi}{2} \leq \theta \leq \frac{\pi}{2},$$

i.e., unit velocity can be assumed.

The system of equations for helix-like geodesic curves (see Fig. 12) $g(x(t), y(t), z(t))$ if $0 < |w| < 1$ is:

$$\begin{aligned} x(t) &= \frac{2c}{w} \sin \frac{wt}{2} \cos \left(\frac{wt}{2} + \alpha \right), \quad y(t) = \frac{2c}{w} \sin \frac{wt}{2} \sin \left(\frac{wt}{2} + \alpha \right), \\ z(t) &= wt \cdot \left\{ 1 + \frac{c^2}{2w^2} \left[\left(1 - \frac{\sin(2wt + 2\alpha) - \sin 2\alpha}{2wt} \right) + \right. \right. \\ &\quad \left. \left. + \left(1 - \frac{\sin(2wt)}{wt} \right) - \left(1 - \frac{\sin(wt + 2\alpha) - \sin 2\alpha}{2wt} \right) \right] \right\} = \\ &= wt \cdot \left\{ 1 + \frac{c^2}{2w^2} \left[\left(1 - \frac{\sin(wt)}{wt} \right) + \left(\frac{1 - \cos(2wt)}{wt} \right) \sin(wt + 2\alpha) \right] \right\}. \end{aligned} \tag{4.8}$$

In the cases with when $w = 0$ the geodesic curve is the following:

$$x(t) = c \cdot t \cos \alpha, \quad y(t) = c \cdot t \sin \alpha, \quad z(t) = \frac{1}{2} c^2 \cdot t^2 \cos \alpha \sin \alpha. \quad (4.9)$$

The cases $|w| = 1$ are trivial: $(x, y) = (0, 0), z = w \cdot t$.

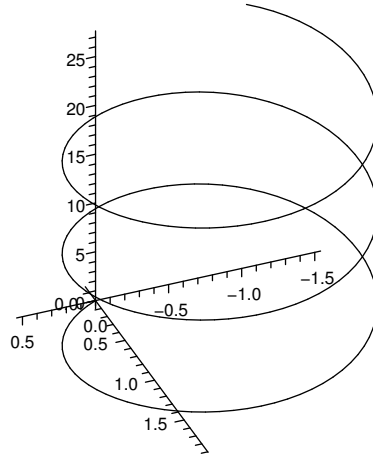


Figure 12. Geodesic curve with parameters $\alpha = \frac{\pi}{6}$ and $\beta = \frac{\pi}{4}$.

Definition 4.3. The distance $d(P_1, P_2)$ between the points P_1 and P_2 is defined by the arc length of geodesic curve from P_1 to P_2 .

Definition 4.4. The geodesic sphere of radius R with centre at the point P_1 is defined as the set of all points P_2 in the space with the condition $d(P_1, P_2) = R$. Moreover, we require that the geodesic sphere is a simply connected surface without self-intersection in Nil space (Fig. 13).

Definition 4.5. The body of the geodesic sphere with centre P_1 and radius R in Nil space is called a geodesic ball, denoted by $B_{P_1}(R)$, i.e., $Q \in B_{P_1}(R)$ if and only if $0 \leq d(P_1, Q) \leq R$.

We proved in [64, 55] the following theorems:

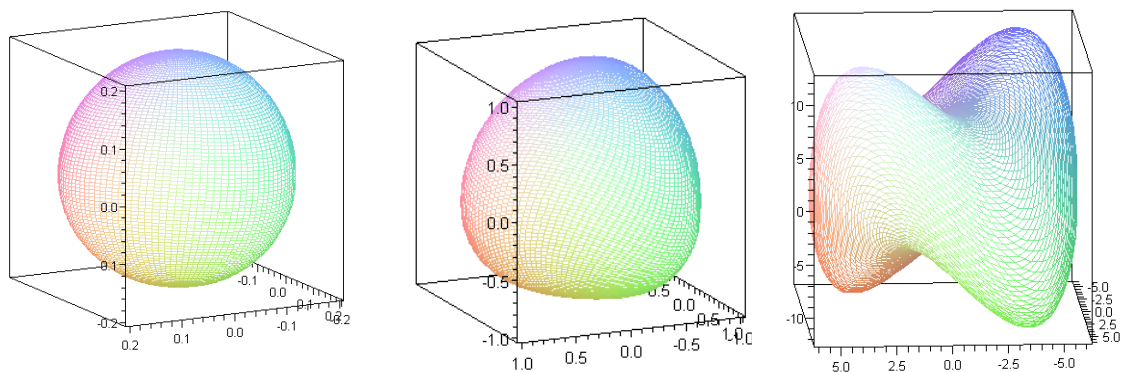


Figure 13. Nil geodesic spheres of radii: $R = 0.2, R = 1, R = 6$.

Theorem 4.6 ([55]). The geodesic sphere and ball of radius R exist in Nil space if and only if $R \in [0, 2\pi]$.

Theorem 4.7 ([64]). *The geodesic Nil ball $B(S(R))$ is convex in the affine-Euclidean sense in our model if and only if $R \in [0, \frac{\pi}{2}]$.*

Next, we recall some important properties of geodesic curves and spheres proved in [67].

1. Consider points $P(x(t), y(t), z(t))$ lying on a sphere S of radius R centred at the origin. The coordinates of P are given by parameters $(\alpha \in [-\pi, \pi), \theta \in [-\frac{\pi}{2}, \frac{\pi}{2}], R > 0)$.

From the equations (4.8) and (4.9) we directly obtain the following

Lemma 4.8 ([67]). *(a) $x(t)^2 + y(t)^2 = \frac{4c^2}{w^2} \sin^2 \frac{wt}{2}$, that is if $\theta \neq \pm \frac{\pi}{2}$ and $t = R$ is given and $\alpha \in [-\pi, \pi)$ then the endpoints P of the geodesic curves lie on a cylinder of radius $r = \left| \frac{4c}{w} \sin \frac{wR}{2} \right|$ with axis z . Therefore, we obtain the following connection between parameters θ and R :*

$$R = 2 \cdot \arcsin \left[\frac{\sqrt{x^2(R) + y^2(R)}}{2 \cdot \cot \theta} \right] \frac{1}{\sin \theta} \tag{4.10}$$

(b) If $\theta = \pm \frac{\pi}{2}$ then the endpoints $P(x(R), y(R), z(R))$ of the geodesics $g(x(t), y(t), z(t))$ lie on the z -axis thus their orthogonal projections onto the $[x, y]$ -plane are the origin and $x(R) = y(R) = 0, z(R) = d(O, R) = R$.

(c) Moreover, the cross section of the spheres S with the plane $[x, z]$ is given by the following system of equations:

$$\begin{aligned} X(R, \theta) &= \frac{2c}{w} \sin \frac{wR}{2} = \frac{2 \cos \theta}{\sin \theta} \sin \frac{R \sin \theta}{2}, \\ Z(R, \theta) &= wR + \frac{c^2 R}{2w} - \frac{c^2}{2w^2} \sin wR = \\ R \sin \theta + \frac{R \cos^2 \theta}{2 \sin \theta} - \frac{\cos^2 \theta}{2 \sin^2 \theta} \sin(R \sin \theta), \quad (\theta \in [-\frac{\pi}{2}, \frac{\pi}{2}] \setminus \{0\}); \\ \text{if } \theta = 0 \text{ then } X(R, 0) &= R, Z(R, 0) = 0. \end{aligned} \tag{4.11}$$

2. In [67] we introduced the usual notion of the fibre projection \mathcal{P} , a projection parallel to fibre lines (parallel to the z -axis) onto the $[x, y]$ plane. The image of a point P is the intersection with the $[x, y]$ base plane of the line parallel to the fibre line passing through $P, \mathcal{P}(P) = P^*$.

Analysing the parametric equations of the geodesic curves $g(x(t), y(t), z(t))$ with starting points at the origin we found the following

Lemma 4.9 ([67]). *If $0 < |w| < 1$ for the geodesic curve $g(x(t), y(t), z(t))$ ($t \in [0, R]$) then the fibre projection \mathcal{P} of the geodesic curves onto the $[x, y]$ plane is an Euclidean circular arc that is contained in a circle with equation*

$$\left(x(t) + \frac{c}{w} \sin \alpha\right)^2 + \left(y(t) - \frac{c}{w} \cos \alpha\right)^2 = \left(\frac{c}{w}\right)^2 = \cot^2 \theta. \tag{4.12}$$

If $w = 0$ then the fibre projection \mathcal{P} of the geodesic curves $g(x(t), y(t), z(t))$ ($t \in [0, R]$) onto the $[x, y]$ plane is a segment with starting point at the origin where it is contained by the straight line with equation

$$y = \tan \alpha \cdot x. \tag{4.13}$$

If $w = 1$ then the fibre projection \mathcal{P} of the geodesic curves $g(x(t), y(t), z(t))$ ($t \in [0, R]$) onto the $[x, y]$ plane is the origin.

From the equation (4.12) we directly have the following

Corollary 4.10 ([67]). *(a) If we know the equation of the circle that contains the orthogonal projected image OP^* of a geodesic curve segment $g_{OP} = g(x(t), y(t), z(t))$ ($t \in [0, R]$) onto the $[x, y]$ plane where $0 < |w| < 1$ is a known real number and the coordinates of $P^* = (x(R), y(R), 0)$ then the parametric equation of the geodesic curve segment g_{OP} is uniquely determined. This means that there is a one-to-one correspondence between the circular arcs OP^* and the geodesic curve segments OP in the above sense.*

(b) If $w = 0$ then the fibre projection \mathcal{P} of the geodesic curve is a segment with starting point at the origin and it is contained in the straight line $y = \tan \alpha \cdot x$, therefore in this situation there is a one-to-one correspondence between the projected image OP^ and the geodesic curve segments OP .*

(c) If $w = 1$ then the fibre projection \mathcal{P} of the geodesic curve is the origin so here it is also a one-to-one correspondence between the projected image and the above geodesic curves.

4.3. Geodesic triangles and their interior angle sums

Similarly to the $S^2 \times \mathbf{R}$ and $H^2 \times \mathbf{R}$ geometries in subsection 3.4 or more generally in Riemannian geometries the angle θ of two intersecting curves can be determined by the metric tensor (g_{ij}) of the considered geometry (see (4.5)) using the formula (3.9) where tangent vectors at their common point are u and v .

It is clear by the above definition of angles and by the metric tensor (4.5), that the angles are the same as the Euclidean angles at the origin by a pull back translation.

We note here that the angle of two intersecting geodesic curves depends on the orientation of the tangent vectors. We will consider the *interior angles* of the triangles that are denoted at the vertex A_i by ω_i ($i \in \{1, 2, 3\}$).

A geodesic triangle is called fibre-like if one of its edges lies on a fibre line. In this section we study the right-angled fibre-like triangles. We can assume without loss of generality that the vertices A_1, A_2, A_3 of a fibre-like right-angled triangle (see Fig. 14.a-b) have the following coordinates:

$$A_1 = (1, 0, 0, 0), A_2 = (1, 0, 0, z^2), A_3 = (1, x^3, 0, z^3 = z^2) \tag{4.14}$$

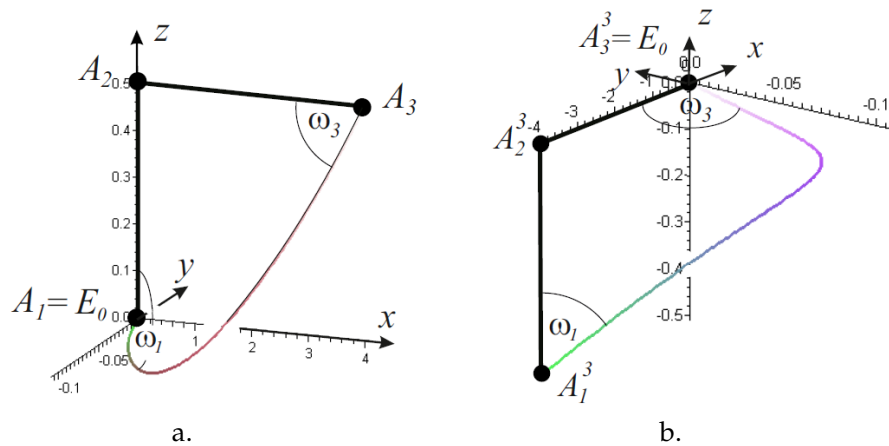


Figure 14. a. The fibre-like geodesic triangle $A_1 A_2 A_3$, where $A_1 = (1, 0, 0, 0)$, $A_2 = (1, 0, 0, \frac{1}{2})$, $A_3 = (1, 4, 0, \frac{1}{2})$. b. Its translated image $A_1^3 A_2^3 A_3^3$ where $A_1^3 = (1, -4, 0, -\frac{1}{2})$, $A_2^3 = (1, -4, 0, 0)$, $A_3^3 = (1, 0, 0, 0)$ (see [58]).

In order to determine the interior angles, we defined translations T_{A_i} , ($i \in \{2, 3\}$) as elements of the isometry group of Nil that maps the origin E_0 onto A_i (see Fig. 14, 15). Our aim is to determine the angle sum $\sum_{i=1}^3 (\omega_i)$ of the interior angles of the above right-angled fibre-like geodesic triangle $A_1 A_2 A_3$. We have seen that $\omega_2 = \frac{\pi}{2}$ and that the angle of geodesic curves with a common point at the origin E_0 is the same as the Euclidean one. Therefore, these angles can be determined in the usual Euclidean sense. Hence, ω_1 is equal to the angle $\angle(g(E_0, A_3), g(E_0, A_2))$ where $g(E_0, A_3)$ and $g(E_0, A_2)$ are oriented geodesic curves. Moreover, the translation T_{A_3} is an isometry in Nil geometry, thus ω_3 is equal to the angle $\angle(g(A_3^3, A_1^3), g(A_3^3, A_2^3))$ where $g(A_3^3, A_1^3)$ and $g(A_3^3, A_2^3)$ are also oriented geodesic curves ($E_0 = A_3^3$).

We denote the oriented unit tangent vectors of the geodesic curves $g(E_0, A_i^j)$ with t_i^j where $(i, j) \in \{(1, 3), (2, 3), (3, 0), (2, 0)\}$ and $A_3^0 = A_3, A_2^0 = A_2$. The Euclidean coordinates of t_i^j are :

$$t_i^j = (\cos(\theta_i^j) \cos(\alpha_i^j), \cos(\theta_i^j) \sin(\alpha_i^j), \sin(\theta_i^j)). \tag{4.15}$$

Lemma 4.11 ([58]). *The sum of the interior angles of a fibre-like right-angled geodesic triangle is greater than or equal to π .*

Conjecture 4.12 ([58]). *The sum of the interior angles of any fibre-like geodesic triangle is greater or equal to π .*

We fix the coordinates the $z^2 = z^3 \in \mathbf{R}$ of A_2 and A_3 and study the interior angle sum $\sum_{i=1}^3 (\omega_i(x^3))$ of the right-angled geodesic triangle $A_1 A_2 A_3$ if the x^3 coordinate of A_3 tends to zero or infinity. E.g. $\lim_{x^3 \rightarrow 0} (\omega_1(x^3)) = 0$ because the geodesic line $g(E_0, A_3)$ tends to the geodesic line $g(E_0, A_2)$ therefore their angle ω_1 tends to zero, and ω_3 tends to $\frac{\pi}{2}$ (see Fig. 14). Similarly the system of equations (4.8) gives the following results

Lemma 4.13 ([58]). *If the coordinates $z^2 = z^3 \in \mathbf{R}$ are fixed then*

$$\lim_{x^3 \rightarrow 0} (\omega_1(x^3)) = 0, \lim_{x^3 \rightarrow 0} (\omega_3(x^3)) = \frac{\pi}{2} \Rightarrow \lim_{x^3 \rightarrow 0} \left(\sum_{i=1}^3 (\omega_i(x^3)) \right) = \pi,$$

$$\lim_{x^3 \rightarrow \infty} (\omega_1(x^3)) = \frac{\pi}{2}, \quad \lim_{x^3 \rightarrow \infty} (\omega_3(x^3)) = 0 \Rightarrow \lim_{x^3 \rightarrow \infty} \left(\sum_{i=1}^3 (\omega_i(x^3)) \right) = \pi.$$

4.3.1. *Hyperbolic-like right angled geodesic triangles* A geodesic triangle is hyperbolic-like if its vertices lie in the base plane of the model. In this section we recall the results of [58] about the interior angle sum of right-angled hyperbolic-like triangles. We can assume without loss of generality that the vertices A_1, A_2, A_3 of a hyperbolic-like right-angled triangle (see Fig. 15) T_g have the following coordinates:

$$A_1 = (1, 0, 0, 0), \quad A_2 = (1, 0, y^2, 0), \quad A_3 = (1, x^3, y^2 = y^3, 0).$$

First we fix the $x^3 \in \mathbf{R}$ coordinate of the vertex A_3 and study the interior angle sum $\sum_{i=1}^3 (\omega_i(y^2 = y^3))$ of the

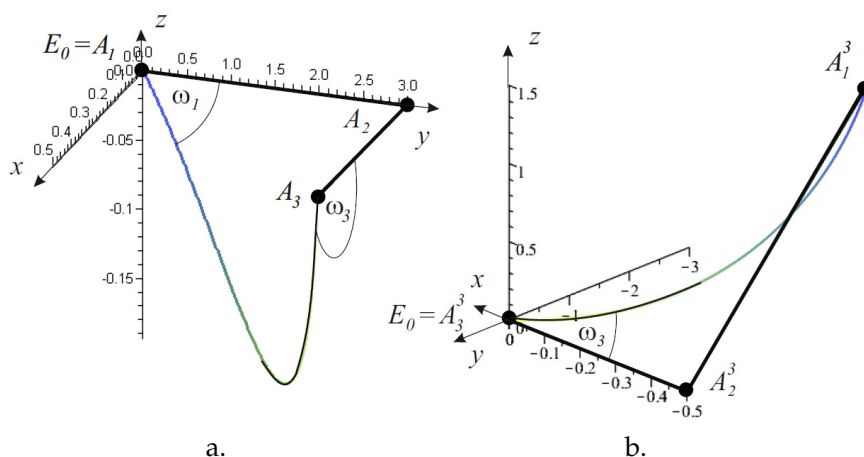


Figure 15. A hyperbolic-like geodesic triangle $A_1 A_2 A_3$, where $A_1 = (1, 0, 0, 0)$, $A_2 = (1, 0, 3, 0)$, $A_3 = (1, \frac{1}{2}, 3, 0)$. b. Its translated image $A_1^3 A_2^3 A_3^3$ where $A_1^3 = (1, -\frac{1}{2}, -3, \frac{3}{2})$, $A_2^3 = (1, -\frac{1}{2}, 0, 0)$, $A_3^3 = (1, 0, 0, 0)$ (see [58]).

right-angled geodesic triangle $A_1 A_2 A_3$ if the coordinates $y^2 = y^3$ of vertices A_2 and A_3 tend to zero or infinity. From the system of equations (4.8) we obtain the following results

Lemma 4.14 ([58]). *If the coordinate $x^3 \in \mathbf{R}$ is fixed then*

$$\lim_{y^2=y^3 \rightarrow 0} (\omega_1(y^2)) = \frac{\pi}{2}, \quad \lim_{y^2=y^3 \rightarrow 0} (\omega_3(y^2)) = 0 \Rightarrow \lim_{y^2=y^3 \rightarrow 0} \left(\sum_{i=1}^3 (\omega_i(y^2)) \right) = \pi,$$

$$\lim_{y^2=y^3 \rightarrow \infty} (\omega_1(y^2)) = 0, \quad \lim_{y^2=y^3 \rightarrow \infty} (\omega_3(y^2)) = \frac{\pi}{2} \Rightarrow \lim_{y^2=y^3 \rightarrow \infty} \left(\sum_{i=1}^3 (\omega_i(y^2)) \right) = \pi.$$

Secondly we fix the $y^2 = y^3 \in \mathbf{R}$ coordinates of the vertices A_2 and A_3 and study the internal angle sum $\sum_{i=1}^3 (\omega_i(x^3))$ of the right-angled geodesic triangle $A_1 A_2 A_3$ if the x^3 coordinate of the vertex A_3 tends to zero or infinity. From the system of equations (4.8) we obtain the following

Lemma 4.15 ([58]). *If the coordinates $y^2 = y^3 \in \mathbf{R}$ are fixed then*

$$\lim_{x^3 \rightarrow 0} (\omega_1(x^3)) = 0, \quad \lim_{x^3 \rightarrow 0} (\omega_3(x^3)) = \frac{\pi}{2} \Rightarrow \lim_{x^3 \rightarrow 0} \left(\sum_{i=1}^3 (\omega_i(x^3)) \right) = \pi,$$

$$\lim_{x^3 \rightarrow \infty} (\omega_1(x^3)) = \frac{\pi}{2}, \quad \lim_{x^3 \rightarrow \infty} (\omega_3(x^3)) = 0 \Rightarrow \lim_{x^3 \rightarrow \infty} \left(\sum_{i=1}^3 (\omega_i(x^3)) \right) = \pi.$$

We can determine the interior angle sum of an arbitrary hyperbolic-like geodesic triangle similarly as in the fibre-like case.

Finally, we have the following

Lemma 4.16 ([58]). *The interior angle sums of hyperbolic-like right-angled geodesic triangles are less than or equal to π .*

Conjecture 4.17 ([58]). *The sum of the interior angles of any hyperbolic-like geodesic triangle is less than or equal to π .*

4.3.2. *Geodesic triangles with interior angle sum π* In the above sections we discussed the fibre- and hyperbolic-like geodesic triangles and proved that there are right-angled geodesic triangles whose angle sum $\sum_{i=1}^3(\omega_i)$ is greater, less than or equal to π , but $\sum_{i=1}^3(\omega_i) = \pi$ is realized if one of the vertices of a geodesic triangle $A_1A_2A_3$ tends to infinity. In [58] we proved the following

Lemma 4.18 ([58]). *There exists a geodesic triangle $A_1A_2A_3$ with interior angle sum π where its vertices are proper (i.e., $A_i \in \text{Nil}$, vertices are not at infinity, $i \in \{1, 2, 3\}$).*

We summarize the lemmas of this Section as follows

Theorem 4.19 ([58]). *The sum of the interior angles of a geodesic triangle of Nil space can be greater, less or equal to π .*

4.4. On Menelaus' and Ceva's theorems in Nil space

As in previous the $S^2 \times \mathbf{R}$ and $H^2 \times \mathbf{R}$ spaces, the question arises as to what the surface of a geodesic triangle will be and which elementary theorems may be true in this geometry. In the paper [67], as in the previously discussed spaces, we introduced the concept of the surface of Nil geodesic triangles using Apollonius surfaces and examined the theorems of Menelaus and Ceva. To discuss Menelaus' and Ceva's theorems, we had to define what we consider to be a *line* on the surface of a geodesic triangle and the definition of a simple ratio.

Let $S_{A_0A_1A_2}$ be the surface of the geodesic triangle $A_0A_1A_2$ and $P_1, P_2 \in S_{A_0A_1A_2}$ be any two points. Natural requirements for a *line* passing through points P_1 and P_2 on $S_{A_0A_1A_2}$ are that:

1. Two surface points uniquely determine a *line* (connecting curve) $\mathcal{G}_{P_1P_2}^{S_{A_0A_1A_2}}$.
2. Any two points on a surface *line* $\mathcal{G}_{P_1P_2}^{S_{A_0A_1A_2}}$ define the same line.
3. The surface *line* determined by two points of a geodesic curve lying on the surface $S_{A_0A_1A_2}$ coincides with the geodesic curve.

Remark 4.20. *An obvious option for definition of a line (connecting curve) $\mathcal{G}_{P_1P_2}^{S_{A_0A_1A_2}}$ would be the fibre projection of the geodesic curve $g_{P_1P_2}$ into the surface $S_{A_0A_1A_2}$ but it is clear that this definition does not satisfy requirement 2.*

We consider a *geodesic triangle* $A_0A_1A_2$ in the projective model of Nil space (see Subsection 4.1). Without loss of generality, we can assume that $A_0 = (1, 0, 0, 0)$. The geodesic lines that contain the sides A_0A_1 and A_0A_2 of the given triangle can be characterized directly by the corresponding parameters θ_i and α_i ($i = 1, 2$) (see (4.8) and (4.9)). The geodesic curve including the side segment A_1A_2 is also determined by one of its endpoints and its parameters. In order to determine the corresponding parameters of this geodesic line we use *for example* a Nil translation $\mathbf{T}(A_1)$, as elements of the isometry group of Nil geometry, that maps $A_1 = (1, x_1, y_1, z_1)$ onto $A_0 = (1, 0, 0, 0)$ (up to a positive determinant factor).

Remark 4.21. *By the results of Theorem 4.6, we may assume that the surface $S_{A_0A_1A_2}$ of the geodesic triangle $A_0A_1A_2$ is contained by a geodesic Nil sphere of radius π .*

We generalized the notion of simple ratio to the triples point lying on geodesic lines of Nil space:

Definition 4.22. Let A, B , and P be distinct points on a geodesic curve in Nil space. Then their simple ratio is

$$s^N(A, P, B) = d(A, P)/d(P, B)$$

if P is between A and B , and

$$s^N(A, P, B) = -d(A, P)/d(P, B)$$

otherwise, where d is the distance function of Nil geometry.

Let A, B and P be distinct points on a non-fibre-like geodesic curve in Nil and let A^*, B^* and P^* be their projected images by \mathcal{P} .

Lemma 4.23 ([67]). *The Euclidean length $C(A^*, P^*)$ of a circle arc or line segment A^*P^* satisfies the following equations*

$$C(A^*, P^*) = d(A, P) \cdot \cos \theta, \quad C(P^*, B^*) = d(P, B) \cdot \cos \theta. \tag{4.16}$$

Therefore, the projection \mathcal{P} preserves the ratio of lengths in the above sense.

Lemma 4.9, Corollary 4.10 and the above projection \mathcal{P} were used to define the surface line but the definition is technical due to the complex structure of the geometry and therefore they are not detailed here (see [67]). The main results are summarized as follows

Corollary 4.24 ([67]). *Menelaus' theorem does not hold in Nil geometry. However, the so-called Menelaus' condition plays an important role in defining lines on the surface of a given triangle (see [67]).*

Using the above Menelaus' condition, similar to the Euclidean proof, we obtain the Nil Ceva's theorem:

Theorem 4.25 ([67]). *If T is a point on a geodesic triangle $A_0A_1A_2$ in Nil space which does not lie on any side such that the curves $\mathcal{G}_{A_0T}^{S_{A_0A_1A_2}}$ and $g_{A_1A_2}$ intersect at P_{12} , $\mathcal{G}_{A_1T}^{S_{A_0A_1A_2}}$ and $g_{A_0A_2}$ at P_{02} , and $\mathcal{G}_{A_2T}^{S_{A_0A_1A_2}}$ and $g_{A_0A_1}$ at P_{01} , then*

$$s^N(A_0, P_{01}, A_1)s^N(A_1, P_{12}, A_2)s^N(A_2, P_{02}, A_0) = 1.$$

Using the Lemma 4.9 it follows that the corresponding Ceva theorem is also true for the projected configuration i.e. for the triangle $A_0^*A_1^*A_2^*$ and the points $T^*, P_{01}^*, P_{12}^*, P_{02}^*$.

Theorem 4.26 ([67]). *If T^* is a point not on any side of circle arc triangle (the projected image of a geodesic triangle in general type) $A_0^*A_1^*A_2^*$ in the base plane of the Nil space such that the arcs (or line segments) $\widehat{A_0^*T^*}$ and $\widehat{A_1^*A_2^*}$ meet in P_{12}^* , $\widehat{A_1^*T^*}$ and $\widehat{A_0^*A_2^*}$ in P_{02}^* , and $\widehat{A_2^*T^*}$ and $\widehat{A_0^*A_1^*}$ in P_{01}^* , then*

$$s^c(A_0^*, P_{01}^*, A_1^*)s^c(A_1^*, P_{12}^*, A_2^*)s^c(A_2^*, P_{02}^*, A_0^*) = 1.$$

Remark 4.27. *Using the previous notions and theorems, as in the Euclidean case, we can define, for example, the circumscribed circle of a geodesic triangle and its centre, the centroid of a geodesic triangle as the point where the three medians of the triangle meet. A median of a geodesic triangle $A_0A_1A_2$ in the Nil space is a surface line $\mathcal{G}^{S_{A_0A_1A_2}}$ from one vertex to the midpoint on the opposite side of the triangle. We will examine these in a forthcoming paper.*

5. $\widetilde{SL_2R}$ geometry

The basic concepts of the model of $\widetilde{SL_2R}$ geometry can be found in [30].

In [9] the authors considered the geodesics and geodesic spheres that gave exact solutions of an ODE system that describes geodesics. Moreover, geodesic spheres are determined and a visualization of $\widetilde{SL_2R}$ geometry is also given. In [10] Z. Erjavec and D. Horvat investigated and characterized the non-geodesic biharmonic curves and proved the statement that only proper biharmonic curves are helices. Also, the explicit parametric equations of proper biharmonic helices were found. In [11] the author derived the equation of a minimal surface and gave fundamental examples of minimal surfaces. In [12] Z. Erjavec discussed the so-called Killing magnetic curves. In [43] the authors discussed visualization methods of the considered geometry.

In [7], we studied the sum of the interior angles of the geodesic and translation triangles (see Subsection 5.3).

5.1. Basic notions of the $\widetilde{SL_2R}$ geometry

In this section we summarize the real 2×2 matrices $\begin{pmatrix} d & b \\ c & a \end{pmatrix}$ with unit determinant $ad - bc = 1$ which constitute a Lie transformation group by the usual product operation, taken to act on row matrices as on point coordinates on the right as follows

$$(z^0, z^1) \begin{pmatrix} d & b \\ c & a \end{pmatrix} = (z^0d + z^1c, z^0b + z^1a) = (w^0, w^1) \tag{5.1}$$

$$\text{with } w = \frac{w^1}{w^0} = \frac{b + \frac{z^1}{z^0}a}{d + \frac{z^1}{z^0}c} = \frac{b + za}{d + zc}$$

as a right action on the complex projective line C^∞ . This group is a 3-dimensional manifold, because of its 3 independent real coordinates and with its usual neighbourhood topology [54], [80]. In order to model the above structure in the projective sphere \mathcal{PS}^3 and in the projective space \mathcal{P}^3 (see [30]), we introduce the new projective coordinates (x^0, x^1, x^2, x^3) where

$$a := x^0 + x^3, \quad b := x^1 + x^2, \quad c := -x^1 + x^2, \quad d := x^0 - x^3.$$

Then it follows that

$$0 > bc - ad = -x^0x^0 - x^1x^1 + x^2x^2 + x^3x^3 \tag{5.2}$$

describes the interior of the above one-sheeted hyperboloid solid \mathcal{H} in the usual Euclidean coordinate simplex, with the origin $E_0(1, 0, 0, 0)$ and the ideal points of the axes $E_1^\infty(0, 1, 0, 0)$, $E_2^\infty(0, 0, 1, 0)$, $E_3^\infty(0, 0, 0, 1)$. We consider the collineation group \mathbf{G}_* that acts on the projective sphere \mathcal{SP}^3 and preserves a polarity, i.e. a scalar product of signature $(- - ++)$, this group leaves the one sheeted hyperboloid solid \mathcal{H} invariant. We have to choose an appropriate subgroup \mathbf{G} of \mathbf{G}_* as the isometry group, then the universal covering group and space $\widetilde{\mathcal{H}}$ of \mathcal{H} will be the hyperboloid model of $\widetilde{\mathbf{SL}}_2\mathbf{R}$ ([30]).

The specific isometries $\mathbf{S}(\phi)$ ($\phi \in \mathbf{R}$) constitute a one parameter group given by the matrices

$$\mathbf{S}(\phi) : (s_i^j(\phi)) = \begin{pmatrix} \cos \phi & \sin \phi & 0 & 0 \\ -\sin \phi & \cos \phi & 0 & 0 \\ 0 & 0 & \cos \phi & -\sin \phi \\ 0 & 0 & \sin \phi & \cos \phi \end{pmatrix}. \tag{5.3}$$

The elements of $\mathbf{S}(\phi)$ are the so-called *fibre translations*. We obtain a unique fibre line to each $X(x^0, x^1, x^2, x^3) \in \widetilde{\mathcal{H}}$ as the orbit by right action of $\mathbf{S}(\phi)$ on X . The coordinates of points lying on the fibre line through X can be expressed as the images of X by $\mathbf{S}(\phi)$:

$$\begin{aligned} (x^0, x^1, x^2, x^3) &\xrightarrow{\mathbf{S}(\phi)} (x^0 \cos \phi - x^1 \sin \phi, x^0 \sin \phi + x^1 \cos \phi, \\ &x^2 \cos \phi + x^3 \sin \phi, -x^2 \sin \phi + x^3 \cos \phi) \end{aligned} \tag{5.4}$$

for the Euclidean coordinate set $x := \frac{x^1}{x^0}, y := \frac{x^2}{x^0}, z := \frac{x^3}{x^0}, x^0 \neq 0$.

In (5.3) and (5.4) we can see the 2π periodicity of ϕ . Moreover, we see the (logical) extension to $\phi \in \mathbf{R}$, as real parameter, to have the universal covers $\widetilde{\mathcal{H}}$ and $\widetilde{\mathbf{SL}}_2\mathbf{R}$, respectively, through the projective sphere \mathcal{PS}^3 . The elements of the isometry group of $\mathbf{SL}_2\mathbf{R}$ (and so by the above extension the isometries of $\widetilde{\mathbf{SL}}_2\mathbf{R}$) can be described by the matrix (a_i^j) (see [30] and [31])

$$\begin{aligned} (a_i^j) &= \begin{pmatrix} a_0^0 & a_0^1 & a_0^2 & a_0^3 \\ \mp a_0^1 & \pm a_0^0 & \pm a_0^3 & \mp a_0^2 \\ a_2^0 & a_2^1 & a_2^2 & a_2^3 \\ \pm a_2^1 & \mp a_2^0 & \mp a_2^3 & \pm a_2^2 \end{pmatrix} \text{ where} \\ &-(a_0^0)^2 - (a_0^1)^2 + (a_0^2)^2 + (a_0^3)^2 = -1, \quad -(a_2^0)^2 - (a_2^1)^2 + (a_2^2)^2 + (a_2^3)^2 = 1, \\ &-a_0^0a_2^0 - a_0^1a_2^1 + a_0^2a_2^2 + a_0^3a_2^3 = 0 = -a_0^0a_2^1 + a_0^1a_2^0 - a_0^2a_2^3 + a_0^3a_2^2, \end{aligned} \tag{5.5}$$

and we allow positive proportionality, as the projective freedom. The horizontal intersection of the hyperboloid solid \mathcal{H} with the plane $E_0E_2^\infty E_3^\infty$ provides the *base plane* of the model $\widetilde{\mathcal{H}} = \widetilde{\mathbf{SL}}_2\mathbf{R}$. The fibre through X intersects the hyperbolic (\mathbf{H}^2) base plane $z^1 = x = 0$ at the foot point

$$Z(z^0 = x^0x^0 + x^1x^1; z^1 = 0; z^2 = x^0x^2 - x^1x^3; z^3 = x^0x^3 + x^1x^2). \tag{5.6}$$

We introduce a so-called hyperboloid parametrization as in [30] as follows

$$\begin{aligned} x^0 &= \cosh r \cos \phi, \\ x^1 &= \cosh r \sin \phi, \\ x^2 &= \sinh r \cos(\theta - \phi), \\ x^3 &= \sinh r \sin(\theta - \phi), \end{aligned} \tag{5.7}$$

where (r, θ) are the polar coordinates of the \mathbf{H}^2 base plane, and ϕ is the fibre coordinate. We note that

$$-x^0x^0 - x^1x^1 + x^2x^2 + x^3x^3 = -\cosh^2 r + \sinh^2 r = -1 < 0.$$

The inhomogeneous coordinates will play an important role in the later E^3 -visualization, e.g., of the prism tilings in $\widetilde{SL}_2\mathbf{R}$, and are given by

$$\begin{aligned} x &= \frac{x^1}{x^0} = \tan \phi, \\ y &= \frac{x^2}{x^0} = \tanh r \frac{\cos(\theta - \phi)}{\cos \phi}, \\ z &= \frac{x^3}{x^0} = \tanh r \frac{\sin(\theta - \phi)}{\cos \phi}. \end{aligned}$$

5.2. Distances and spheres

The infinitesimal arc length square can be derived by the standard pull back method. By the T^{-1} -action of (5.6) on the differentials $(dx^0; dx^1; dx^2; dx^3)$, we obtain that in this parametrization the infinitesimal arc length square at any point of $\widetilde{SL}_2\mathbf{R}$ is the following:

$$(ds)^2 = (dr)^2 + \cosh^2 r \sinh^2 r (d\theta)^2 + [(d\phi) + \sinh^2 r (d\theta)]^2. \quad (5.8)$$

Hence we get the symmetric metric tensor field g_{ij} on $\widetilde{SL}_2\mathbf{R}$ by components:

$$g_{ij} := \begin{pmatrix} 1 & 0 & 0 \\ 0 & \sinh^2 r (\sinh^2 r + \cosh^2 r) & \sinh^2 r \\ 0 & \sinh^2 r & 1 \end{pmatrix}, \quad (5.9)$$

and

$$dV = \sqrt{\det(g_{ij})} dr d\theta d\phi = \frac{1}{2} \sinh(2r) dr d\theta d\phi$$

as the volume element in the hyperboloid coordinates. The geodesic curves of $\widetilde{SL}_2\mathbf{R}$ are generally defined as having locally minimal arc length between any two of their (close enough) points.

By (5.9) the second order differential equation system of the $\widetilde{SL}_2\mathbf{R}$ geodesic curve is the following:

$$\begin{aligned} \ddot{r} &= \sinh(2r) \dot{\theta} \dot{\phi} + \frac{1}{2} (\sinh(4r) - \sinh(2r)) \dot{\theta} \dot{\theta}, \\ \ddot{\phi} &= 2\dot{r} \tanh(r) (2\sinh^2(r) \dot{\theta} + \dot{\phi}), \\ \ddot{\theta} &= \frac{2\dot{r}}{\sinh(2r)} ((3 \cosh(2r) - 1) \dot{\theta} + 2\dot{\phi}). \end{aligned} \quad (5.10)$$

We can assume, by the homogeneity, that the starting point of a geodesic curve is the origin $(1, 0, 0, 0)$. Moreover, $r(0) = 0$, $\phi(0) = 0$, $\theta(0) = 0$, $\dot{r}(0) = \cos(\alpha)$, $\dot{\phi}(0) = \sin(\alpha) = -\dot{\theta}(0)$ are the initial values in Table 1 for the solution of (5.10), and so the unit velocity will be achieved.

Table 2	
Types	
$0 \leq \alpha < \frac{\pi}{4}$ (\mathbf{H}^2 – like direction)	$r(s, \alpha) = \operatorname{arsinh}\left(\frac{\cos \alpha}{\sqrt{\cos 2\alpha}} \sinh(s\sqrt{\cos 2\alpha})\right)$ $\theta(s, \alpha) = -\arctan\left(\frac{\sin \alpha}{\sqrt{\cos 2\alpha}} \tanh(s\sqrt{\cos 2\alpha})\right)$ $\phi(s, \alpha) = 2 \sin \alpha s + \theta(s, \alpha)$
$\alpha = \frac{\pi}{4}$ (light direction)	$r(s, \alpha) = \operatorname{arsinh}\left(\frac{\sqrt{2}}{2} s\right)$ $\theta(s, \alpha) = -\arctan\left(\frac{\sqrt{2}}{2} s\right)$ $\phi(s, \alpha) = \sqrt{2}s + \theta(s, \alpha)$
$\frac{\pi}{4} < \alpha \leq \frac{\pi}{2}$ (fibre – like direction)	$r(s, \alpha) = \operatorname{arsinh}\left(\frac{\cos \alpha}{\sqrt{-\cos 2\alpha}} \sin(s\sqrt{-\cos 2\alpha})\right)$ $\theta(s, \alpha) = -\arctan\left(\frac{\sin \alpha}{\sqrt{-\cos 2\alpha}} \tan(s\sqrt{-\cos 2\alpha})\right)$ $\phi(s, \alpha) = 2 \sin \alpha s + \theta(s, \alpha)$

The equation of geodesic curve in the hyperboloid model was determined in [9], with the usual geographical sphere coordinates (λ, α) , $(-\pi < \lambda \leq \pi, -\frac{\pi}{2} \leq \alpha \leq \frac{\pi}{2})$, and the arc length parameter $0 \leq s \in \mathbf{R}$.

Definition 5.1. The distance $d(P_1, P_2)$ between the points P_1 and P_2 is defined by the arc length of the geodesic curve from P_1 to P_2 .

Definition 5.2. The geodesic sphere of radius ρ (denoted by $S_{P_1}(\rho)$) with centre at point P_1 is defined as the set of all points P_2 satisfying the condition $d(P_1, P_2) = \rho$. Moreover, we require that the geodesic sphere is a simply connected surface without self-intersection (Fig. 16).

Definition 5.3. The body of the geodesic sphere of centre P_1 and radius ρ is called geodesic ball, denoted by $B_{P_1}(\rho)$, i.e., $Q \in B_{P_1}(\rho)$ if and only if $0 \leq d(P_1, Q) \leq \rho$.

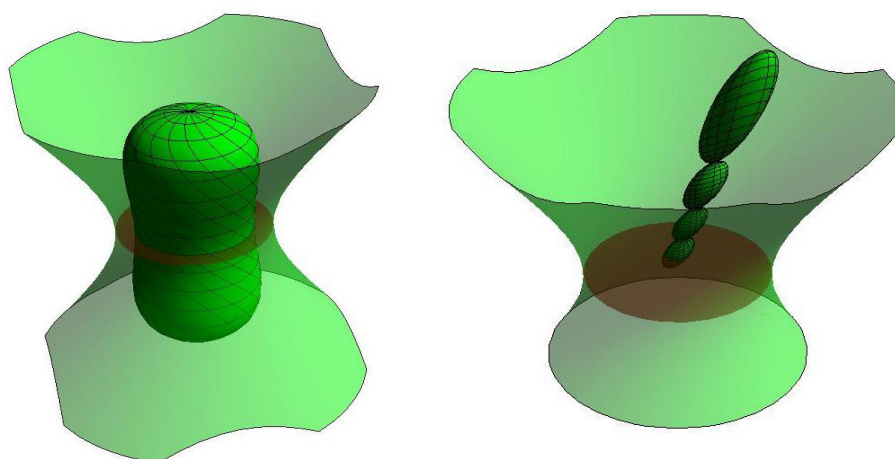


Figure 16. a. Geodesic sphere of radius 1 centred at the origin, b. A series of tangent geodesic spheres of radius $\frac{1}{6}$ centred along a fibre line.

From (5.10) and from Table 2 it follows that $S(\rho)$ is a simply connected surface in both \mathbf{E}^3 and $\widetilde{\mathbf{SL}}_2\mathbf{R}$ if $\rho \in [0, \frac{\pi}{2})$. If $\rho \geq \frac{\pi}{2}$ then the universal cover should be discussed. Therefore, we consider geodesic spheres and balls only with radii $\rho \in [0, \frac{\pi}{2})$ in the following. These will be satisfactory in our cases.

5.3. Geodesic triangles and their interior angle sums

In this subsection we recall the results of [7].

5.3.1. *Fibre-like right angled triangles* A geodesic triangle is called fibre-like if one of its edges lies on a fibre line (Fig. 17). We can assume without loss of generality that the vertices A_1, A_2, A_3 of a fibre-like right angled triangle T_g has the following coordinates: $A_1 = (1, 0, 0, 0)$, $A_2 = (1, 0, y^2, 0)$, $A_3 = (1, x^3, 0, 0)$.

The geodesic segment A_1A_2 lies on the y axis, the geodesic segment A_1A_3 lies on the x axis and its angle is $\omega_1 = \frac{\pi}{2}$ in $\widetilde{\mathbf{SL}}_2\mathbf{R}$ (this angle is also $\frac{\pi}{2}$ in the Euclidean sense since $A_1 = E_0$).

In order to determine the further interior angles of the fibre-like geodesic triangle $A_1A_2A_3$ we define translations $\mathbf{T}_{A_i}, (i \in \{2, 3\})$ as elements of the isometry group of $\widetilde{\mathbf{SL}}_2\mathbf{R}$, that maps the origin E_0 onto A_i . E.g., the isometry \mathbf{T}_{A_2} and its inverse (up to a positive determinant factor) and the images $\mathbf{T}_{A_2}(A_i)$ of the vertices $A_i (i \in \{1, 2, 3\})$ are the following:

$$\begin{aligned} \mathbf{T}_{A_2}^{-1}(A_1) = A_1^2 &= (1, 0, -y^2, 0), \quad \mathbf{T}_{A_2}^{-1}(A_2) = A_2^2 = E_0 = (1, 0, 0, 0), \\ \mathbf{T}_{A_2}^{-1}(A_3) = A_3^2 &= (1, x^3, -y^2, x^3y^2). \end{aligned} \tag{5.11}$$

Similarly to the above cases we obtain:

$$\begin{aligned} \mathbf{T}_{A_3}^{-1}(A_1) = A_1^3 &= (1, -x^3, 0, 0), \quad \mathbf{T}_{A_3}^{-1}(A_2) = A_2^3 = (1, -x^3, y^2, -x^3y^2), \\ \mathbf{T}_{A_3}^{-1}(A_3) = A_3^3 &= E_0 = (1, 0, 0, 0). \end{aligned} \tag{5.12}$$

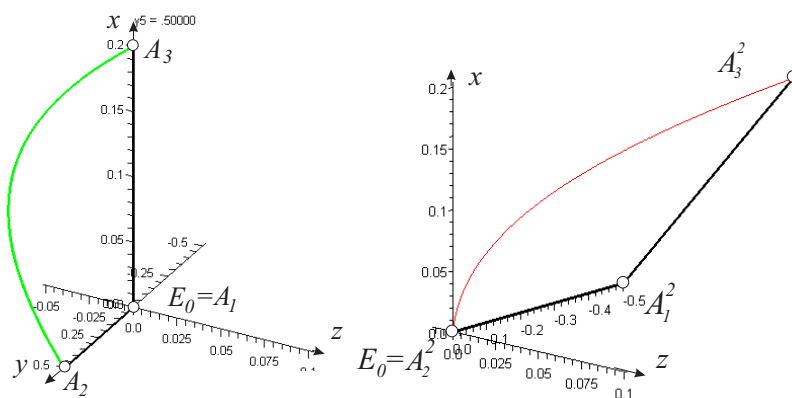


Figure 17. A fibre-like geodesic triangle $A_1A_2A_3$ and its translated image $A_1^2A_2^2A_3^2$ by translation \mathbf{T}_{A_2}

Lemma 5.4 ([7]). *The sum of the interior angles of a fibre-like right angled geodesic triangle is greater or equal to π .*

5.3.2. *Hyperbolic-like right angled geodesic triangles* A geodesic triangle is hyperbolic-like if its vertices lie in the base plane (i.e., in the $[y, z]$ coordinate plane) of the model. In this section we analyze the interior angle sum of the right angled hyperbolic-like triangles. We can assume without loss of generality that the vertices A_1, A_2, A_3 of a hyperbolic-like right angled triangle (see Figure 18) T_g have the following coordinates: $A_1 = (1, 0, 0, 0)$, $A_2 = (1, 0, y^2, 0)$, $A_3 = (1, 0, 0, z^3)$. The geodesic segment A_1A_2 lies on the y axis, the geodesic segment A_1A_3 lies on the z axis and its angle is $\omega_1 = \frac{\pi}{2}$ in the $\widetilde{\mathbf{SL}}_2\mathbf{R}$ space (this angle is in the Euclidean sense also $\frac{\pi}{2}$ since $A_1 = E_0$).

Similarly we get to the above cases that the images $\mathbf{T}_{A_j}^{-1}(A_i)$ of the vertices $A_i (i \in \{1, 2, 3\}, j \in \{2, 3\})$ are the following (see also Figure 18):

$$\begin{aligned} \mathbf{T}_{A_2}^{-1}(A_1) = A_1^2 &= (1, 0, -y^2, 0), \quad \mathbf{T}_{A_2}^{-1}(A_2) = A_2^2 = E_0 = (1, 0, 0, 0), \\ \mathbf{T}_{A_2}^{-1}(A_3) = A_3^2 &= (1, y^2z^3, -y^2, z^3), \end{aligned} \tag{5.13}$$

$$\begin{aligned} \mathbf{T}_{A_3}^{-1}(A_1) = A_1^3 &= (1, -z^3, 0, 0), \quad \mathbf{T}_{A_3}^{-1}(A_2) = A_2^3 = (1, -y^2z^3, y^2, -z^3), \\ \mathbf{T}_{A_3}^{-1}(A_3) = A_3^3 &= E_0 = (1, 0, 0, 0), \end{aligned} \tag{5.14}$$

Finally, we obtain the following lemma:

Lemma 5.5 ([7]). *The interior angle sums of hyperbolic-like geodesic triangles can be less than or equal to π .*

Conjecture 5.6 ([7]). *The interior angle sum of any hyperbolic-like right angled geodesic triangle is less Than or equal to π .*

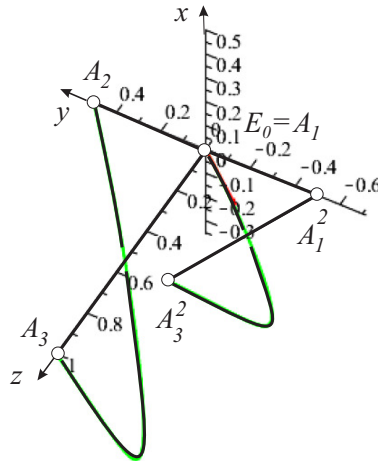


Figure 18. A hyperbolic-like geodesic triangle $A_1 A_2 A_3$ and its translated copy $A_1^2 A_2^2 A_3^2$

5.3.3. *Geodesic triangles with interior angle sum π* In the above sections we discussed the fibre- and hyperbolic-like geodesic triangles and proved that there are right angled geodesic triangles whose angle sum $\sum_{i=1}^3(\omega_i)$ is greater than or equal to π , less than or equal to π , but $\sum_{i=1}^3(\omega_i) = \pi$ is realized only if one of the vertices of a geodesic triangle $A_1 A_2 A_3$ tends to infinity (see Table 3-4). We prove the following

Lemma 5.7 ([7]). *There is geodesic triangle $A_1 A_2 A_3$ with interior angle sum π where its vertices are proper (i.e. $A_i \in \widetilde{\mathbf{SL}}_2\mathbf{R}$).*

We summarize the lemmas of this Section as follows

Theorem 5.8 ([7]). *The sum of the interior angles of a geodesic triangle of $\widetilde{\mathbf{SL}}_2\mathbf{R}$ can be greater, less or equal to π .*

6. Sol space

The projective model of Sol geometry was developed in [30].

6.1. Basic notions of Sol geometry

In this section we summarize the significant concepts and notations of real Sol geometry (see [30], [54]).

Sol is defined as a 3-dimensional real Lie group with multiplication

$$(a, b, c)(x, y, z) = (x + ae^{-z}, y + be^z, z + c). \tag{6.1}$$

We note that conjugation by (x, y, z) leaves invariant the plane (a, b, c) with fixed c :

$$(x, y, z)^{-1}(a, b, c)(x, y, z) = (x(1 - e^{-c}) + ae^{-z}, y(1 - e^c) + be^z, c). \tag{6.2}$$

Moreover, for $c = 0$ the action of (x, y, z) is only by its z -component, where $(x, y, z)^{-1} = (-xe^z, -ye^{-z}, -z)$. Thus the $(a, b, 0)$ plane is distinguished as a *base plane* in Sol, or in other words, $(x, y, 0)$ is a normal subgroup of Sol. Sol multiplication can also be affinely (projectively) interpreted by "right translations" on its points as the following matrix formula shows, according to (6.1):

$$(1; a, b, c) \rightarrow (1; a, b, c) \begin{pmatrix} 1 & x & y & z \\ 0 & e^{-z} & 0 & 0 \\ 0 & 0 & e^z & 0 \\ 0 & 0 & 0 & 1 \end{pmatrix} = (1; x + ae^{-z}, y + be^z, z + c) \tag{6.3}$$

by row-column multiplication. This defines "translations" $\mathbf{L}(\mathbf{R}) = \{(x, y, z) : x, y, z \in \mathbf{R}\}$ on the points of the space $\mathbf{Sol} = \{(a, b, c) : a, b, c \in \mathbf{R}\}$. These translations are not commutative, in general. Here we can consider \mathbf{L} as a projective collineation group with right actions in homogeneous coordinates as usual in classical affine-projective geometry. We will use the Cartesian homogeneous coordinate simplex $E_0(\mathbf{e}_0), E_1^\infty(\mathbf{e}_1), E_2^\infty(\mathbf{e}_2)$,

$E_3^\infty(\mathbf{e}_3)$, $(\{e_i\} \subset \mathbf{V}^4$ with the unit point $E(e = \mathbf{e}_0 + \mathbf{e}_1 + \mathbf{e}_2 + \mathbf{e}_3)$) which is distinguished by an origin E_0 and by the ideal points of coordinate axes, respectively. Thus Sol can be visualized in the affine 3-space \mathbf{A}^3 (so in Euclidean space \mathbf{E}^3) as well (see [60]).

In this affine-projective context E. Molnár in [30] derived the usual infinitesimal arc length square at any point of Sol, by pull back translation, as follows

$$(ds)^2 := e^{2z}(dx)^2 + e^{-2z}(dy)^2 + (dz)^2. \tag{6.4}$$

Hence we get the infinitesimal Riemannian metric invariant under translations, by the symmetric metric tensor field g on Sol by components as usual.

It will be important for us that the full isometry group $Isom(\text{Sol})$ has eight components, since the stabilizer of the origin is isomorphic to the dihedral group \mathbf{D}_4 , generated by two involutive (involutory) transformations, preserving (6.4):

(1) $y \leftrightarrow -y$; (2) $x \leftrightarrow y$; $z \leftrightarrow -z$; i.e. first by 3×3 matrices :

$$(1) \begin{pmatrix} 1 & 0 & 0 \\ 0 & -1 & 0 \\ 0 & 0 & 1 \end{pmatrix}; \quad (2) \begin{pmatrix} 0 & 1 & 0 \\ 1 & 0 & 0 \\ 0 & 0 & -1 \end{pmatrix}; \tag{6.5}$$

with its product, generating a cyclic group \mathbf{C}_4 of order 4

$$\begin{pmatrix} 0 & 1 & 0 \\ -1 & 0 & 0 \\ 0 & 0 & -1 \end{pmatrix}; \quad \begin{pmatrix} -1 & 0 & 0 \\ 0 & -1 & 0 \\ 0 & 0 & 1 \end{pmatrix}; \quad \begin{pmatrix} 0 & -1 & 0 \\ 1 & 0 & 0 \\ 0 & 0 & -1 \end{pmatrix}; \quad \mathbf{Id} = \begin{pmatrix} 1 & 0 & 0 \\ 0 & 1 & 0 \\ 0 & 0 & 1 \end{pmatrix}.$$

Or we write by collineations fixing the origin $O(1, 0, 0, 0)$:

$$(1) \begin{pmatrix} 1 & 0 & 0 & 0 \\ 0 & 1 & 0 & 0 \\ 0 & 0 & -1 & 0 \\ 0 & 0 & 0 & 1 \end{pmatrix}, \quad (2) \begin{pmatrix} 1 & 0 & 0 & 0 \\ 0 & 0 & 1 & 0 \\ 0 & 1 & 0 & 0 \\ 0 & 0 & 0 & -1 \end{pmatrix} \text{ of form (6.5).} \tag{6.6}$$

A general isometry of Sol is defined by a product $\gamma_O \tau_X$, first γ_O of the form (6.6) then τ_X of the form (6.3). For a general point $A(1, a, b, c)$, this will be a product $\tau_A^{-1} \gamma_O \tau_X$, mapping A into $X(1, x, y, z)$.

Conjugated translation τ by the above isometry γ , are denoted as $\tau^\gamma = \gamma^{-1} \tau \gamma$.

6.2. Related results in Sol geometry

In the paper [4] the authors considered the geodesics and Frenet formulas in Sol space, gave the differential equation system that describes geodesics but unfortunately the differential equation system in the main cases cannot be expressed with elementary functions.

Therefore, the Sol geodesic sphere unfortunately cannot be expressed in a closed explicit form. We could visualize the geodesic sphere by numerically solving differential equations (see Fig. 19). In [13] Z. Erjavec

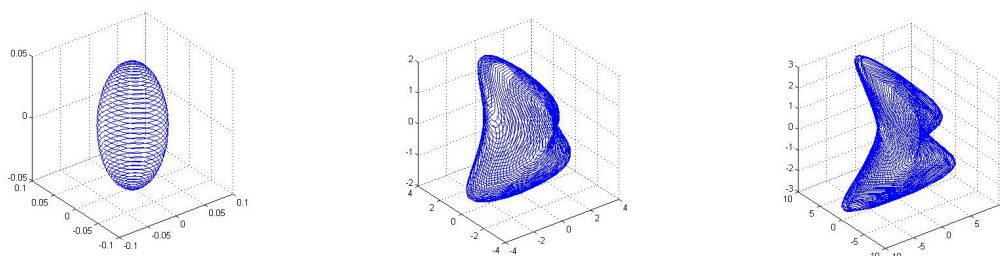


Figure 19. Sol geodesic balls of radii $R = 0.05$, $R = 2$, $R = 3$.

studied certain class of Weingarten surfaces. The main result is that the only non-planar ruled Weingarten surfaces composed from vertical geodesics are the surfaces $r(u, v) = (ae^{ku}, be^{-ku}, v)$. In [15] the authors determined magnetic curves corresponding to the Killing magnetic fields in Sol. In [14] Z. Erjavec and J.

Inoguchi discussed magnetic curves with respect to the almost cosymplectic structure and investigated the curvature properties of these curves.

In [36] we classified Sol lattices in an algorithmic way with 17 types, in analogy with the 14 Bravais types of Euclidean 3-lattices, but infinitely many Sol affine equivalence classes in each type. Then the discrete isometry groups of compact fundamental domain (crystallographic groups) can also be classified into infinitely many classes but finitely many types. For this we studied relations between Sol lattices and lattices of the pseudoeuclidean (or here rather called Minkowskian) plane. Moreover, we introduced the notion of Sol parallelepiped to every lattice type.

In [8] we studied a series of 2-generator Sol-manifolds depending on a positive integer n constructed as tetrahedron manifolds, and proved that they are twofold coverings of the 3-sphere branched over specified links.

7. Ball packings in Thurston geometries

7.1. Geodesic ball packings in spaces of constant curvature

Let X denote a space of constant curvature, either the n -dimensional sphere S^n , Euclidean space E^n , or hyperbolic space H^n with $n \geq 2$. An important question of discrete geometry is to find the highest possible packing density in X by congruent non-overlapping balls of a given radius [1], [18].

Euclidean cases are the best explored. One major recent development has been the settling of the long-standing Kepler conjecture, part of Hilbert's 18th problem, by Thomas Hales at the turn of the 21st century. Hales' computer-assisted proof was largely based on a program set forth by L. Fejes Tóth in the 1950's [21].

In n -dimensional hyperbolic geometry several new questions occur concerning packing and covering problems, e.g., in H^n there are 3 kinds of "generalized balls (spheres)": the *usual balls* (spheres), *horoballs* (horospheres) and *hyperballs* (hyperspheres). Moreover, the definition of packing density is crucial in hyperbolic spaces as shown by Böröczky [2]. For standard examples also see [1], [18]. The most widely accepted notion of packing density considers the local densities of balls with respect to their Dirichlet–Voronoi cells (cf. [2]). In order to consider ball packings in \bar{H}^n , we use an extended notion of such local density.

In space X^n let $d_n(r)$ be the density of $n + 1$ mutually touching spheres or horospheres of radius r (in case of horosphere $r = \infty$) with respect to the simplex spanned by their centres. L. Fejes Tóth and H. S. M. Coxeter conjectured that the packing density of balls of radius r in X^n cannot exceed $d_n(r)$. This conjecture has been proved by C. A. Rogers for the Euclidean space E^n . The 2-dimensional spherical case was settled by L. Fejes Tóth in [20].

In [2] K. Böröczky proved the following theorem for *ball and horoball* packings for any dimension $2 \leq n \in \mathbf{N}$:

In an n -dimensional space of constant curvature, consider a packing of spheres of radius r . In spherical space suppose that $r < \frac{\pi}{4}$. Then the density of each sphere in its Dirichlet–Voronoi cell cannot exceed the density of $n + 1$ spheres of radius r mutually touching one another with respect to the simplex spanned by their centres.

This density is ≈ 0.85328 in H^3 which is not realized by packings with equal balls. However, it is attained by the horoball packing (case $r = \infty$) of \bar{H}^3 where the ideal centres of horoballs lie on the absolute figure of \bar{H}^3 . This corresponds to packing an ideal regular tetrahedron tiling given by the Coxeter–Schläfli symbol $\{3, 3, 6\}$. Ball packings of hyperbolic n -space and of other Thurston geometries are extensively discussed in the literature see e.g. [1, 18, 19, 35], where the reader finds further references as well.

In this survey, we do not deal in detail with the examination of the ball (sphere) packings and coverings of spaces of constant curvature, so now we only mention that the questions regarding horosphere and hypersphere packings and coverings are not yet settled. New interesting problems have also arisen, the examination of which are related to the use of Busemann functions. The interested reader can read about the results of these in the papers [16, 24, 25, 26, 27, 69, 70, 71, 72, 73, 74, 75, 76, 77, 78, 79] and the references therein.

7.2. Geodesic ball packings in Thurston geometries of non-constant curvature

Definitions of ball (sphere) packing and covering densities are already critical in hyperbolic geometry, therefore in order to introduce this concept to Thurston geometries of non-constant curvature we use the discrete isometry groups of the considered geometry. First, we have summarized the basic definitions and notions of this (see [56]).

Let X be one of the five Thurston geometries with non-constant curvature

$$\mathbf{S}^2 \times \mathbf{R}, \mathbf{H}^2 \times \mathbf{R}, \widetilde{\mathbf{SL}}_2\mathbf{R}, \mathbf{Nil}, \mathbf{Sol},$$

where the geodesic curves are generally defined as having locally minimal arc length between any two of their points (sufficiently close to each other). The system of equations for the parametrized geodesic curves $\gamma(\tau)$ in our model can be determined by the general theory of Riemannian geometry. Then a geodesic sphere and ball can usually be defined as follows. We consider only geodesic ball packings which are transitively generated by discrete groups of isometries of X and the density of the packing is related to its Dirichlet–Voronoi cells.

In the following, let Γ be a fixed group of isometries of X . Denote by $d(P_1, P_2)$ the distance of two points P_1, P_2 .

Definition 7.1. We say that the point set

$$\mathcal{D}(K) = \{P \in X : d(K, P) \leq d(K^{\mathbf{g}}, P) \text{ for all } \mathbf{g} \in \Gamma\}$$

is the Dirichlet–Voronoi cell ($D - V$ cell) of Γ around the kernel point $K \in X$.

Definition 7.2. We say that

$$\Gamma_P = \{\mathbf{g} \in \Gamma : P^{\mathbf{g}} = P\}$$

is the stabilizer subgroup of $P \in X$ in Γ .

Definition 7.3. Assume that the stabilizer $\Gamma_K = \mathbf{I}$ is the identity, i.e., Γ acts simply transitively on the Γ -orbit of $K \in X$. Then let B_K denote the largest ball with centre K inside the $D - V$ cell $\mathcal{D}(K)$. Moreover, let $\rho(K)$ denote the radius of B_K . It is easy to see that

$$\rho(K) = \min_{\mathbf{g} \in \Gamma \setminus \mathbf{I}} \frac{1}{2}d(K, K^{\mathbf{g}}).$$

Definition 7.4. If the stabilizer $\Gamma_K > \mathbf{I}$ then Γ acts multiply transitively on the Γ -orbit of $K \in X$. In this case the greatest ball radius of B_K is

$$\rho(K) = \min_{\mathbf{g} \in \Gamma \setminus \Gamma_K} \frac{1}{2}d(K, K^{\mathbf{g}}),$$

where K belongs to a 0-, 1-, or 2-dimensional region of X (vertices, axes, reflection planes).

In both cases the Γ -images of B_K form a ball packing \mathcal{B}_K^Γ with centre points $K^{\mathbf{g}}$.

Definition 7.5. The density of ball packing \mathcal{B}_K^Γ is

$$\delta(K) = \frac{\text{Vol}(B_K)}{\text{Vol}(\mathcal{D}(K))}.$$

It is clear that the orbit K^Γ and the ball packing \mathcal{B}_K^Γ have the same symmetry group. Moreover, this group contains the crystallographic group Γ :

$$\text{Sym}K^\Gamma = \text{Sym}\mathcal{B}_K^\Gamma \geq \Gamma.$$

Definition 7.6. We say that the orbit K^Γ and the ball packing \mathcal{B}_K^Γ are characteristic if $\text{Sym}K^\Gamma = \Gamma$, otherwise the orbit and the ball packing are not characteristic.

7.2.1. Simply transitive ball packings Let Γ be a fixed group of isometries in the space X . Our goal is to find a point $K \in X$ and the orbit K^Γ for Γ such that $\Gamma_K = \mathbf{I}$ and the density $\delta(K)$ of the corresponding ball packing $\mathcal{B}^\Gamma(K)$ is maximal. In this case the ball packing $\mathcal{B}^\Gamma(K)$ is said to be optimal.

We have to determine the maximal radius $\rho(K)$ of the balls, and the maximal density $\delta(K)$. The space groups considered could have free parameters. So we have to find the densest ball packing for fixed parameters $p(\Gamma)$, and then we have to vary $p(\Gamma)$ to get the optimal ball packing

$$\delta(\Gamma) = \max_{K, p(\Gamma)} (\delta(K)). \tag{7.1}$$

We look for the optimal kernel point in a 3-dimensional region, contained in a fundamental domain of Γ .

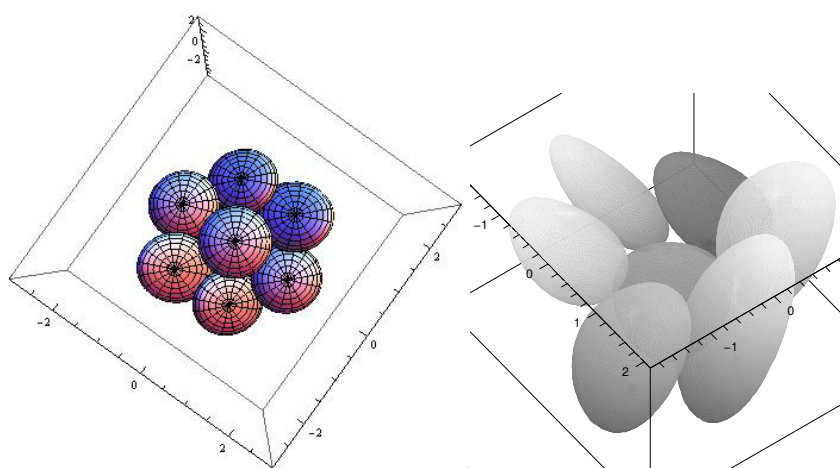


Figure 20. The densest geodesic lattice-like geodesic ball packing in Nil space.

7.2.2. *Multiply transitive ball packings* Similarly to the simply transitive case we must find a kernel point $K \in X$ and the orbit K^Γ of Γ such that the density $\delta(K)$ of the corresponding ball packing $\mathcal{B}^\Gamma(K)$ is maximal, but here $\Gamma_K \neq \mathbf{I}$. Such a ball packing $\mathcal{B}^\Gamma(K)$ is also called *optimal*. In this multiply transitive case we look for the optimal kernel point K in possible 0-, 1-, or 2-dimensional regions \mathcal{L} , respectively. Our aim is to determine the maximal radius $\rho(K)$ of the balls, and the maximal density $\delta(K)$. The space group considered can also have free parameters $p(\Gamma)$. Then we find the densest ball packing for fixed parameters, and vary them to find the optimal ball packing

$$\delta(\Gamma) = \max_{K \in \mathcal{L}, p(\Gamma)} (\delta(K)). \quad (7.2)$$

7.2.3. *Geodesic ball packings in Nil* W. Heisenberg's famous real matrix group provides a non-commutative translation group of an affine 3-space. Nil geometry, which is one of the eight homogeneous Thurston 3-geometries, can be derived from this matrix group (see Section 4).

In [55] we investigated the geodesic balls of Nil and computed their volume, introduced the notion of the Nil lattice, Nil parallelepiped and the density of the lattice-like ball packing. Moreover, we have determined the densest lattice-like geodesic ball packing by a family of Nil lattices. The density of this packing is ≈ 0.78085 , which may be surprising enough in comparison with the 3-dimensional analogous Euclidean result $\frac{\pi}{\sqrt{18}} \approx 0.74048$. The kissing number of every ball in this packing is 14 (Fig. 20, 21). *We conjecture that in Nil space the densest geodesic ball packing belongs to the above ball arrangement.* The symmetry group of this packing has also been described in [31]. In [53] we investigated the geodesic ball packings related to Nil prism tilings where we found that the largest density is ≈ 0.7272 and the kissing number of this ball arrangement is again 14.

7.2.4. *Geodesic ball packings in $\mathbf{H}^2 \times \mathbf{R}$* This Seifert fibre space is derived from the direct product of the hyperbolic plane \mathbf{H}^2 and the real line \mathbf{R} . In [63] we determined the geodesic balls of $\mathbf{H}^2 \times \mathbf{R}$ and computed their volume, defined the notion of the geodesic ball packing and its density. Moreover, we have developed a procedure to determine the density of the simply or multiply transitive geodesic ball packings for generalized Coxeter space groups of $\mathbf{H}^2 \times \mathbf{R}$ and applied this algorithm to them. For the above space groups the Dirichlet-Voronoi cells are "prisms" in the $\mathbf{H}^2 \times \mathbf{R}$ sense. The optimal packing density of the generalized Coxeter space groups is ≈ 0.60726 . I am sure, that in this space there are denser ball packings.

7.2.5. *Geodesic ball packings in $\widetilde{\mathbf{SL}}_2\mathbf{R}$ space* In [68] we investigated the regular prisms and prism tilings in $\widetilde{\mathbf{SL}}_2\mathbf{R}$ (see Section 5) and in [38] we considered the problem of geodesic ball packings related to tilings and their symmetry groups $\mathfrak{pq}2_1$. Moreover, we computed the volumes of prisms and defined the notion of geodesic ball packing and its density. In [38] we developed a procedure to determine the densities of the densest geodesic ball packings for the tilings considered, more precisely, for their generating groups $\mathfrak{pq}2_1$ (for integer rotational parameters p, q ; $3 \leq p, \frac{2p}{p-2} < q$). We looked for those parameters p and q above, where the packing density as largest as possible. Currently our record is 0.5674 for $(p, q) = (8, 10)$. In [59] we studied the non-periodic geodesic ball packings related to the prism tilings and of the cases examined, the highest density that occurs is ≈ 0.6266 .

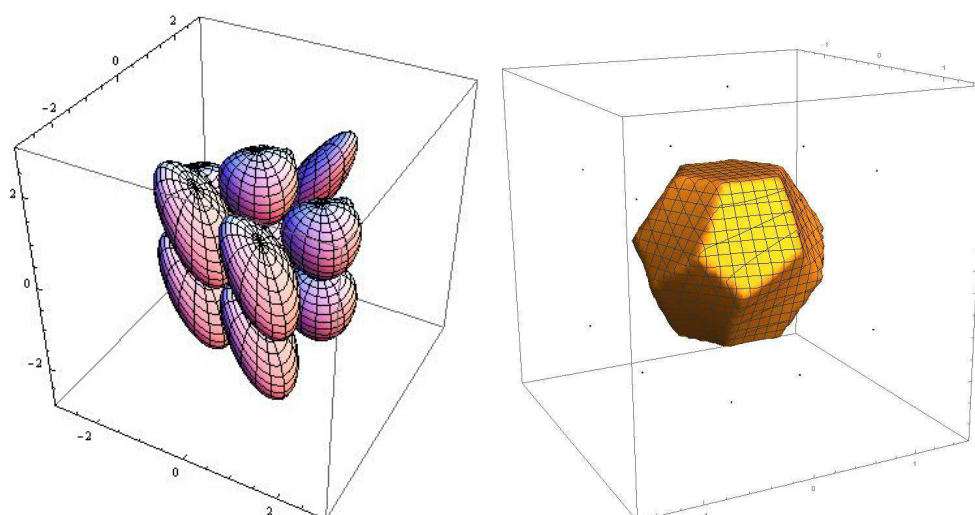


Figure 21. The densest geodesic lattice-like geodesic ball packing in Nil space and the corresponding Dirichlet-Voronoi cell.

In [40] we considered tilings $\mathcal{T}(p, (q, k), (o, \ell))$ for suitable integer positive parameters p, q, k, o, ℓ . Every tiling \mathcal{T} is generated by discrete isometry group $\mathbf{pq}_k\mathbf{o}_\ell$ for $k = 1, o = 2, \ell = 1$. That means this group is generated by a p -rotation \mathbf{p} about the central fibre, then by \mathbf{q}_k screw with q -rotation and $\frac{k}{q}$ translation, then by an \mathbf{o}_ℓ screw with o -rotation and $\frac{\ell}{o}$ translation, just by Euclidean analogy but exact projective computations. We computed the maximal density of the ball packings induced by the $\mathbf{pq}_k\mathbf{o}_\ell$ group action for any parameters. In the next Table 3 we have summarized some numerical results with the top density ≈ 0.787758 . The table contain the optimal radius ρ_{opt} , the volume of the ball $B(\rho_{\text{opt}})$, the volume of the prism \mathcal{P}_p , and the packing density $\delta(\rho_{\text{opt}})$ that is the ratio of the preceding volumes.

Table 3. Geodesic ball packings above in $\widetilde{\text{SL}}_2\mathbf{R}$ for $\mathbf{pq}_k\mathbf{o}_\ell$ with $k = 1, o = 2, \ell = 1$.

q	p	ρ_{opt}	$\text{vol}(B(\rho_{\text{opt}}))$	$\text{vol}(\mathcal{P}_p)$	$\delta(\rho_{\text{opt}})$
3	8	0.392699	0.266949	0.411234	0.635408
3	9	0.521044	0.647905	0.822467	0.787758
3	10	0.599849	1.017248	1.315947	0.773016
4	5	0.314159	0.134202	0.246740	0.543899
4	6	0.501354	0.573426	0.822467	0.697203
4	7	0.613204	1.092403	1.586186	0.688698
5	4	0.261799	0.076892	0.164493	0.467450
5	5	0.485013	0.516444	0.822467	0.627920
5	6	0.614925	1.102375	1.754596	0.628278

7.3. Geodesic ball packings in $\mathbf{S}^2 \times \mathbf{R}$ space

The structure and the model of $\mathbf{S}^2 \times \mathbf{R}$ geometry are described in Sections 2-3.

In this section we briefly show the structure of the discrete isometry groups of the $\mathbf{S}^2 \times \mathbf{R}$ geometry, through which we can see that there are analogies with the Euclidean case, but even this geometry exhibits significant differences.

The points in the $\mathbf{S}^2 \times \mathbf{R}$ geometry are described by (P, p) where $P \in \mathbf{S}^2$ and $p \in \mathbf{R}$. The isometry group $\text{Isom}(\mathbf{S}^2 \times \mathbf{R})$ of $\mathbf{S}^2 \times \mathbf{R}$ can be derived from the direct product of the isometry group of the spherical plane $\text{Isom}(\mathbf{S}^2)$ and the isometry group of the real line $\text{Isom}(\mathbf{R})$. The structure of an isometry group $\Gamma \subset \text{Isom}(\mathbf{S}^2 \times \mathbf{R})$ is the following: $\Gamma = \{(A_1 \times \rho_1), \dots, (A_n \times \rho_n)\}$, where $A_i \times \rho_i := A_i \times (R_i, r_i) := (g_i, r_i)$, ($i \in \{1, 2, \dots, n\}$) and $A_i \in \text{Isom}(\mathbf{S}^2)$, R_i is either the identity map $\mathbf{1}_\mathbf{R}$ of \mathbf{R} or the point reflection $\bar{\mathbf{1}}_\mathbf{R}$. $g_i := A_i \times R_i$ is called the linear part of the transformation $(A_i \times \rho_i)$ and r_i is its translation part. The multiplication formula is the following:

$$(A_1 \times R_1, r_1) \circ (A_2 \times R_2, r_2) = (A_1 A_2 \times R_1 R_2, r_1 R_2 + r_2). \tag{7.3}$$

A group of isometries $\Gamma \subset Isom(\mathbf{S}^2 \times \mathbf{R})$ is called space group if the linear parts form a finite group Γ_0 called the point group of Γ . Moreover, the translation components of the identity of this point group are required to form a one-dimensional lattice L_Γ of \mathbf{R} .

In [17] J. Z. Farkas classified and gave the complete list of the space groups in $\mathbf{S}^2 \times \mathbf{R}$.

In [61] we studied the geodesic balls and their volumes in $\mathbf{S}^2 \times \mathbf{R}$, moreover I have introduced the notion of geodesic ball packing and its density and determined the densest simply and multiply transitive geodesic ball packings for generalized Coxeter space groups of $\mathbf{S}^2 \times \mathbf{R}$, respectively. The density of the densest packing is ≈ 0.82445 .

In the paper [62] we studied the simply transitive locally optimal ball packings for the $\mathbf{S}^2 \times \mathbf{R}$ space groups with Coxeter point groups such that at least one of the generators is a non-trivial glide reflection. We determined the densest simply transitive geodesic ball arrangements for the above space groups, moreover computed their optimal densities and radii. The density of the densest packing in this case is ≈ 0.80408 .

In this survey we only recall the results from [56] where we studied the class of $\mathbf{S}^2 \times \mathbf{R}$ space groups **4q. I. 2** (with a natural parameter $q \geq 2$, see [17]). Each of them belongs to the glide reflection groups, i.e., the generators \mathbf{g}_i ($i = 1, 2, \dots, m$) of its point group Γ_0 are reflections and at least one of the possible translation components of the above generators differs from zero (see [62]).

7.3.1. A very dense multiply transitive ball packing in $\mathbf{S}^2 \times \mathbf{R}$ geometry We considered an $\mathbf{S}^2 \times \mathbf{R}$ space group (see [17, 61, 62] with point group Γ_0 generated by three reflections \mathbf{g}_i ($i = 1, 2, 3$))

$$\begin{aligned} & (+, 0, [] \{(2, 2, q)\}), \quad q \geq 2, \\ \Gamma_0 = & (\mathbf{g}_1, \mathbf{g}_2, \mathbf{g}_3 - \mathbf{g}_1^2, \mathbf{g}_2^2, \mathbf{g}_3^2, (\mathbf{g}_1\mathbf{g}_3)^2, (\mathbf{g}_2\mathbf{g}_3)^2, (\mathbf{g}_1\mathbf{g}_2)^q). \end{aligned}$$

The possible translation parts τ_1, τ_2, τ_3 of the corresponding generators of Γ_0 are derived from the so-called Frobenius congruence relations:

$$(\tau_1, \tau_2, \tau_3) \cong (0, 0, 0), (0, 0, \frac{1}{2}), (\frac{1}{2}, \frac{1}{2}, \frac{1}{2}), (\frac{1}{2}, \frac{1}{2}, 0), (0, \frac{1}{2}, 0), (0, \frac{1}{2}, \frac{1}{2}).$$

If $(\tau_1, \tau_2, \tau_3) \cong (0, 0, \frac{1}{2})$ then we have obtained the $\mathbf{S}^2 \times \mathbf{R}$ space group **4q. I. 2** (for a fixed $q, 2 \leq q \in \mathbf{N}$).

The fundamental domain of the point group of the space group considered is a spherical triangle $A_1A_2A_3$ with angles $\frac{\pi}{q}, \frac{\pi}{2}, \frac{\pi}{2}$ in the base plane. It can be assumed that the fibre coordinate of the centre of the optimal ball is zero and it is a point of the triangle $A_1A_2A_3$.

We consider ball packings related to parameter $q = 2$.

To determine the optimal multiply transitive ball packing we studied 2-cases:

1. K is an interior point of the spherical geodesic segment A_2A_3 (or A_1A_3). In this situation the point K and its images by $\Gamma = \mathbf{4q. I. 2}$ ($q = 2$), as the centres of the optimal ball arrangement $\mathcal{B}_{opt}(K, R)$, have to satisfy some requirements (not detailed here, see [56]), since an arbitrary ball of the optimal packing is fixed by its neighbouring balls. Here we got the optimal packing if $K = A_2$ (or $K = A_1$) with the following data:

$$\begin{aligned} \phi_3 = \frac{\pi}{2} \approx & 1.57079633, \quad \theta_3 = 0, \quad R_3 = \frac{\pi}{2} \approx 1.57079633, \\ Vol(B(R_3)) \approx & 13.74539472, \quad \delta(R_3, K_3) \approx 0.69634983. \end{aligned} \tag{7.4}$$

2. $K = A_3$. Fig. 22 shows the orbit of the point $K = A_3$ by the space group considered. The images of K lie on a line through the origin and A_3 .

$$\begin{aligned} \phi_4 = \frac{\pi}{4} \approx & 0.78539816, \quad \theta_4 = \frac{\pi}{2} \approx 1.57079633, \quad R_4 \approx 1.81379936, \\ Vol(B(R_4)) \approx & 20.00238509, \quad \delta(R_4, K_4) \approx 0.87757183. \end{aligned} \tag{7.5}$$

The "outwardly transformed" images of the balls surround the initial balls (see Fig. 22) thus the touching number of this packing is 4 (see [56]). Finally, we obtain the following

Theorem 7.7 ([56]). *The ball arrangement $\mathcal{B}_{opt}(R_4, K_4)$ provides the densest multiply transitive ball packing of the $\mathbf{S}^2 \times \mathbf{R}$ space group **4q. I. 2** ($q = 2$).*

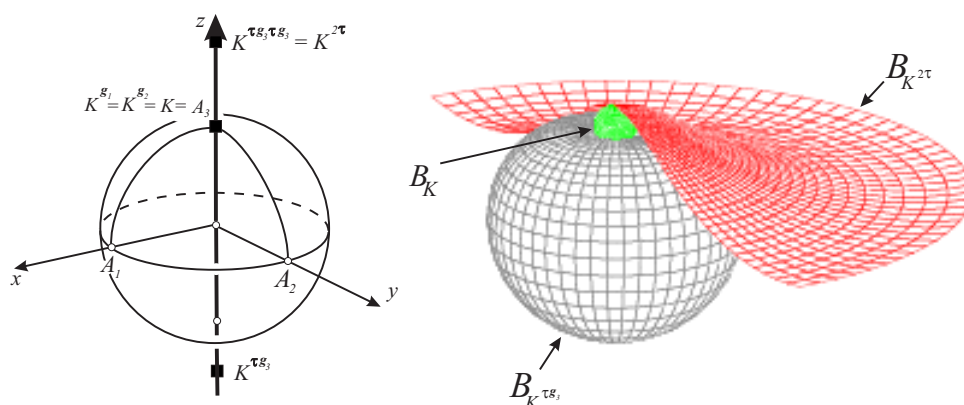


Figure 22. a. The orbit of $K = A_3$ by the group $\Gamma = 4q. I. 2$ ($q = 2$ and τ is the translation part of the group). b. The densest ball packing is determined by its balls $B_K, B_{K^{\tau g_3}}$ and a part of the sphere $B_{K^{2\tau}}$.

Remark 7.8. 1. To the author’s best knowledge there are no results for the geodesic ball packings in Sol geometry at the time of writing.

2. In Nil, $\widetilde{SL}_2\mathbf{R}$ and Sol spaces we have studied the so-called translation ball packings [37, 39, 57, 60, 64, 81] but we did not consider these cases in this work.

7.3.2. The conjecture for the densest ball arrangement in Thurston geometries We introduced the density function for the geodesic ball packings generated by a discrete group of isometries in a given Thurston geometry. This density is related to the Dirichlet–Voronoi cells generated by the centres of balls. For these ball packings we can formulate the following

Conjecture 7.9 ([56]). Let \mathcal{B} be an arbitrary congruent geodesic ball packing in a Thurston geometry X , where \mathcal{B} is generated by a discrete isometry group of X . The above determined ball arrangement $\mathcal{B}_{opt}(R_4, K_4)$ with density $\delta(R_4, K_4) \approx 0.87757183$ provides the densest congruent geodesic ball packing for the Thurston geometries.

The general definition of the density of congruent geodesic ball packings for the Thurston geometries is not settled yet. However, by our investigation for any “good” definition of density the following conjecture may be formulated.

Conjecture 7.10 ([56]). The densest congruent geodesic ball packing in the Thurston geometries is realized by the above ball arrangement $\mathcal{B}_{opt}(R_4, K_4)$ with density $\delta(R_4, K_4) \approx 0.87757183$.

Acknowledgements

In this paper we mentioned only some classical theorems and problems related to Thurston spaces, but we hope that from these the reader can appreciate that our projective method is suitable to study and solve similar problems that represent a huge class of open mathematical problems. Detailed studies are the objective of ongoing research.

Funding

There is no funding for this work.

Availability of data and materials

All data generated or analysed during this study are included in this published article.

Author’s contributions

Authors read and approved the final manuscript.

References

[1] Bezdek, K.: Sphere Packings Revisited. Eur. J. Combin. **27**/6, 864–883 (2006).
 [2] Böröczky, K.: Packing of spheres in spaces of constant curvature. Acta Math. Acad. Sci. Hungar. **32**, 243-261 (1978).

- [3] Brodaczewska, K.: Elementargeometrie in Nil. Dissertation (Dr. rer. nat.) Fakultät Mathematik und Naturwissenschaften der Technischen Universität Dresden (2014).
- [4] Bölskei, A., Szilágyi, B.: *Frenet Formulas and Geodesics in Sol Geometry*. Beitr. Algebra Geom. **48/2**, 411-421 (2007).
- [5] Chavel, I.: *Riemannian Geometry: A Modern Introduction*. Cambridge Studies in Advances Mathematics, Cambridge (2006).
- [6] Cheeger, J., Ebin, D.G.: *Comparison Theorems in Riemannian Geometry*. American Mathematical Society. (2006).
- [7] Csima, G., Szirmai, J.: *Interior angle sum of translation and geodesic triangles in $\widetilde{SL}_2\mathbf{R}$ space*. Filomat. **32/14**, 5023–5036 (2018).
- [8] Cavichioli, A., Molnár, E., Spaggiari, F., Szirmai, J.: *Some tetrahedron manifolds with Sol geometry*. J. Geometry. **105/3**, 601-614 (2014).
- [9] Divjak, B., Erjavec, Z., Szabolcs, B., Szilágyi, B.: *Geodesics and geodesic spheres in $\widetilde{SL}_2\mathbf{R}$ geometry*. Math. Commun. **14/2**, 413-424 (2009).
- [10] Erjavec, Z., Horvat, D.: *Biharmonic curves in $\widetilde{SL}_2\mathbf{R}$ space*. Math. Commun. **19** (2), 291-299 (2014).
- [11] Erjavec, Z.: *Minimal surfaces in $\widetilde{SL}_2\mathbf{R}$ space*. Glas. Mat. Ser. III. **50**, 207-221 (2015).
- [12] Erjavec, Z.: *On Killing magnetic curves in $\widetilde{SL}_2\mathbf{R}$ geometry*. Rep. Math. Phys. **84** (3), 333-350 (2019).
- [13] Erjavec, Z.: *On a certain class of Weingarten surfaces in Sol space*. Int. J. Appl. Math. **28** (5), 507-514 (2015).
- [14] Erjavec, Z., Inoguchi, J.: *On magnetic curves in almost cosymplectic Sol space*. Results Math. **75:113**, 16 pg (2020).
- [15] Erjavec, Z., Inoguchi, J.: *Killing magnetic curves in Sol space*. Math. Phys. Anal. Geom., **21:15**, 15 pg (2018).
- [16] Eper, M., Szirmai, J.: *Coverings with congruent and non-congruent hyperballs generated by doubly truncated Coxeter orthoschemes*. Contributions to Discrete Mathematics. **17** No.2, 23-40 (2022), <https://doi.org/10.11575/cdm.v17i2>.
- [17] Farkas, Z. J.: *The classification of $S^2 \times \mathbf{R}$ space groups*. Beitr. Algebra Geom. **42**, 235-250 (2001).
- [18] Fejes Tóth, G., Kuperberg, W.: *Packing and Covering with Convex Sets*, Handbook of Convex Geometry Volume B, eds. Gruber, P.M., Willis J.M., pp. 799-860, North-Holland, (1983).
- [19] Fejes Tóth, G., Kuperberg, G., Kuperberg, W.: *Highly Saturated Packings and Reduced Coverings*. Monatsh. Math. **125/2**, 127-145 (1998).
- [20] Fejes Tóth, L.: *Regular Figures*, Macmillan New York, 1964.
- [21] Hales, T. C.: *Historical Overview of the Kepler Conjecture*. Discrete and Computational Geometry, **35**, 5-20 (2006).
- [22] Inoguchi, J.: *Minimal translation surfaces in the Heisenberg group Nil₃*. Geom. Dedicata **161/1**, 221-231 (2012).
- [23] Kobayashi, S., Nomizu, K.: *Foundation of differential geometry, I*. Interscience, Wiley, New York (1963).
- [24] Kozma, R. T., Szirmai, J.: *Optimally dense packings for fully asymptotic Coxeter tilings by horoballs of different types*. Monatsh. Math. **168/1**, 27-47 (2012).
- [25] Kozma, R. T., Szirmai, J.: *New Lower Bound for the Optimal Ball Packing Density of Hyperbolic 4-space*. Discrete Comput. Geom. **53/1**, 182-198 (2015), <https://doi.org/10.1007/s00454-014-9634-1>.
- [26] Kozma, R. T., Szirmai, J.: *New horoball packing density lower bound in hyperbolic 5-space*. Geom. Dedicata. **206/1**, 1-25 (2020), <https://doi.org/10.1007/s10711-019-00473-x>.
- [27] Kozma, R. T., Szirmai, J.: *Horoball Packing Density Lower Bounds in Higher Dimensional Hyperbolic n-space for $6 \leq n \leq 9$* . Geom. Dedicata. (2023), <https://doi.org/10.1007/s10711-023-00779-x>.
- [28] Kurusa, Á.: *Ceva's and Menelaus' theorems in projective-metric spaces*. J. Geom. **110/2**, (2019), <https://doi.org/10.1007/s00022-019-0495-x>.
- [29] Manzano, M.J., Torralbo, F.: *New Examples of Constant Mean Curvature Surfaces in SXR and HXR*. Michigan Math. J. **63**, 701-723 (2014).
- [30] Molnár, E.: *The projective interpretation of the eight 3-dimensional homogeneous geometries*. Beitr. Algebra Geom. **38** No. 2, 261-288 (1977).
- [31] : Molnár, E., Szirmai, J.: *Symmetries in the 8 homogeneous 3-geometries*. Symmetry Cult. Sci. **21/1-3**, 87-117 (2010).
- [32] Molnár, E., Szilágyi, B.: *Translation curves and their spheres in homogeneous geometries*. Publ. Math. Debrecen. **78/2**, 327-346 (2010).
- [33] Molnár, E.: *On projective models of Thurston geometries, some relevant notes on Nil orbifolds and manifolds*. Sib. Electron. Math. Izv. **7**, 491-498 (2010), <http://mi.mathnet.ru/semr267>.
- [34] Molnár, E., Szirmai, J.: *On Nil crystallography*. Symmetry Cult. Sci. **17/1-2**, 55-74 (2006).
- [35] Molnár, E., Szirmai, J.: *Top dense hyperbolic ball packings and coverings for complete Coxeter orthoscheme groups*. Publications de l'Institut Mathématique. **103(117)**, 129-146 (2018), <https://doi.org/10.2298/PIM1817129M>.
- [36] Molnár, E., Szirmai, J.: *Classification of Sol lattices*. Geom. Dedicata. **161/1**, 251-275 (2012).
- [37] Molnár, E., Szirmai, J., Vesnin, A.: *Projective metric realizations of cone-manifolds with singularities along 2-bridge knots and links*. J. Geom. **95**, 91-133 (2009).
- [38] Molnár, E., Szirmai, J.: *Volumes and geodesic ball packings to the regular prism tilings in $\widetilde{SL}_2\mathbf{R}$ space*. Publ. Math. Debrecen. **84(1-2)**, 189-203 (2014).
- [39] Molnár, E., Szirmai, J., Vesnin, A.: *Packings by translation balls in $\widetilde{SL}_2\mathbf{R}$* . J. Geom. **105(2)**, 287-306 (2014).
- [40] Molnár E., Szirmai J., Vesnin A.: *Geodesic and Translation Ball Packings Generated by Prismatic Tessellations of the Universal Cover of $\widetilde{SL}_2\mathbf{R}$* . Results in Math. **71**, 623-642 (2017).
- [41] Morabito, F., Rodriguez, M. M.: *Classification of rotational special Weingarten surfaces of minimal type in $S^2 \times \mathbf{R}$ and $H^2 \times \mathbf{R}$* . Mathematische Zeitschrift. **273** (1-2), 379-399 (2013), <https://doi.org/10.1007/s00209-012-1010-3>.
- [42] Németh, L.: *Pascal pyramid in the space $H^2 \times \mathbf{R}$* . Mathematical Communications. **22**, 211-225 (2017).
- [43] Novello, T., da Silva, V., Velhoa, L.: *Visualization of Nil, Sol, and $\widetilde{SL}_2\mathbf{R}$ geometries*. Computers and Graphics. **91**, 219-231 (2020).
- [44] Ohshika K., Papadopoulos, A. (editors): *In the Tradition of Thurston Geometry and Topology*, Springer International Publishing. (2020), ISBN:978-3-030-55927-4.
- [45] Pallagi, J., Schultz, B., Szirmai, J.: *Visualization of geodesic curves, spheres and equidistant surfaces in $S^2 \times \mathbf{R}$ space*. KoG. **14**, 35-40 (2010).
- [46] Pallagi, J., Schultz, B., Szirmai, J.: *Equidistant surfaces in Nil space*. Stud. Univ. Zilina, Math. Ser. **25**, 31-40 (2011).
- [47] Pallagi, J., Schultz, B., Szirmai, J.: *Equidistant surfaces in $H^2 \times \mathbf{R}$ space*. KoG. **15**, 3-6 (2011).
- [48] Pallagi, J., Szirmai, J.: *Visualization of the Dirichlet-Voronoi cells in $S^2 \times \mathbf{R}$ space*. Pollack Periodica. **7** Supp 1, 95–104 (2012), <https://doi.org/10.1556/Pollack.7.2012.S.9>.
- [49] Papadopoulos, A., Su, W.: *On hyperbolic analogues of some classical theorems in spherical geometry*. hal-01064449 (2014).
- [50] Rodriguez, M. M.: *Minimal surfaces with limit ends in $H^2 \times \mathbf{R}$* . Journal für die reine und angewandte Mathematik (Crelle's Journal). **685**, 123-141 (2013), <https://doi.org/10.1515/crelle-2012-0010>.
- [51] Schultz B., Molnár E.: *Geodesic lines and spheres, densest(?) geodesic ball packing in the new linear model of Nil geometry*. Proceedings of the Czech-Slovak Conference on Geometry and Graphics. 177-186 (2015), ISBN 978-80-227-4479-9.

- [52] Schultz, B., Szirmai, J.: *On parallelehedra of Nil-space*. Pollack Periodica. 7. Supp 1, 129-136 (2012).
- [53] Schultz, B., Szirmai, J.: *Geodesic ball packings generated by regular prism tilings in Nil geometry* Miskolc Math. Notes. 23/1, 429-442 (2012), <https://doi.org/10.18514/MMN.2022.2959>.
- [54] Scott, P.: *The geometries of 3-manifolds*. Bull. London Math. Soc. 15, 401-487 (1983).
- [55] Szirmai, J.: *The densest geodesic ball packing by a type of Nil lattices*. Beitr. Algebra Geom. 48(2), 383-398 (2007).
- [56] Szirmai, J.: *A candidate to the densest packing with equal balls in the Thurston geometries*. Beitr. Algebra Geom. 55(2), 441-452 (2014).
- [57] Szirmai, J.: *Lattice-like translation ball packings in Nil space*. Publ. Math. Debrecen. 80(3-4), 427-440 (2012).
- [58] Szirmai, J.: *Nil geodesic triangles and their interior angle sums*. Bull. Braz. Math. Soc. (N.S.) 49, 761-773 (2018).
- [59] Szirmai, J.: *Non-periodic geodesic ball packings to infinite regular prism tilings in $SL(2, \mathbb{R})$ space*. Rocky Mountain Journal of Mathematics. 46/3, 1055-1070 (2016).
- [60] Szirmai, J.: *Bisector surfaces and circumscribed spheres of tetrahedra derived by translation curves in Sol geometry*. New York J. Math. 25, 107-122 (2019).
- [61] Szirmai, J.: *Simply transitive geodesic ball packings to $\mathbb{S}^2 \times \mathbb{R}$ space groups generated by glide reflections*. Ann. Mat. Pur. Appl., 193/4, 1201-1211 (2014), <https://doi.org/10.1007/s10231-013-0324-z>.
- [62] Szirmai, J.: *Geodesic ball packings in $\mathbb{S}^2 \times \mathbb{R}$ space for generalized Coxeter space groups*. Beitr. Algebra Geom. 52, 413 - 430 (2011).
- [63] Szirmai, J.: *Geodesic ball packings in $\mathbb{H}^2 \times \mathbb{R}$ space for generalized Coxeter space groups*. Math. Commun. 17/1, 151-170 (2012).
- [64] Szirmai, J.: *The densest translation ball packing by fundamental lattices in Sol space*. Beitr. Algebra Geom. 51(2), 353-373 (2010).
- [65] Szirmai, J.: *Interior angle sums of geodesic triangles in $\mathbb{S}^2 \times \mathbb{R}$ and $\mathbb{H}^2 \times \mathbb{R}$ geometries*. Bul. Acad. de Stiinte Republicii Mold. Mat. 93(2), 44-61 (2020).
- [66] Szirmai, J.: *Apollonius surfaces, circumscribed spheres of tetrahedra, Menelaus' and Ceva's theorems in $\mathbb{S}^2 \times \mathbb{R}$ and $\mathbb{H}^2 \times \mathbb{R}$ geometries*. Q. J. Math. 73, 477-494 (2022), <https://doi.org/10.1093/qmath/haab038>.
- [67] Szirmai, J.: *On Menelaus' and Ceva's theorem in Nil geometry*. Acta Univ. Sapientiae Math. (2023), arXiv: 2110.08877.
- [68] Szirmai, J.: *Regular prism tilings in $\widetilde{SL}_2\mathbb{R}$ space* Aequat. Math. 88 (1-2), 67-79 (2014), <https://doi.org/10.1007/s00010-013-0221-y>
- [69] Szirmai, J.: *Hyperball packings in hyperbolic 3-space*. Mat. Vesn., 70/3, 211-221 (2018).
- [70] Szirmai, J.: *Packings with horo- and hyperballs generated by simple frustum orthoschemes*. Acta Math. Hungar. 152/2, 365-382 (2017), <https://doi.org/10.1007/s10474-017-0728-0>.
- [71] Szirmai, J.: *Density upper bound of congruent and non-congruent hyperball packings generated by truncated regular simplex tilings*. Rendiconti del Circolo Matematico di Palermo Series 2, 67, 307-322 (2018), <https://doi.org/10.1007/s12215-017-0316-8>.
- [72] Szirmai, J.: *Decomposition method related to saturated hyperball packings*. Ars Math. Contemp., 16, 349-358 (2019).
- [73] Szirmai, J.: *The optimal ball and horoball packings to the Coxeter honeycombs in the hyperbolic d-space*. Beitr. Algebra Geom. 48/1, 35-47 (2007).
- [74] Szirmai, J.: *Horoball packings to the totally asymptotic regular simplex in the hyperbolic n-space*. Aequat. Math. 85, 471-482 (2013), <https://doi.org/10.1007/s00010-012-0158-6>.
- [75] Szirmai, J.: *Horoball packings and their densities by generalized simplicial density function in the hyperbolic space*. Acta Math. Hungar. 136/1-2, 39-55 (2012), <https://doi.org/10.1007/s10474-012-0205-8>.
- [76] Szirmai, J.: *The p-gonal prism tilings and their optimal hypersphere packings in the hyperbolic 3-space*. Acta Math. Hungar. 111 (1-2), 65-76 (2006).
- [77] Szirmai, J.: *The regular prism tilings and their optimal hyperball packings in the hyperbolic n-space*. Publ. Math. Debrecen. 69 (1-2), 195-207 (2006).
- [78] Szirmai, J.: *The optimal hyperball packings related to the smallest compact arithmetic 5-orbifolds*. Kragujevac J. Math. 40(2), 260-270 (2016), <https://doi.org/10.5937/KgJMath1602260S>.
- [79] Szirmai, J.: *The least dense hyperball covering to the regular prism tilings in the hyperbolic n-space*. Ann. Mat. Pur. Appl. 195/1, 235-248 (2016), <https://doi.org/10.1007/s10231-014-0460-0>.
- [80] Thurston, W. P. (and Levy, S. editor): *Three-Dimensional Geometry and Topology*. Princeton University Press, Princeton, New Jersey, vol. 1 (1997).
- [81] Vráncs, A., Szirmai, J.: *Lattice coverings by congruent translation balls using translation-like bisector surfaces in Nil Geometry*. KoG. 23, 6-17 (2019).
- [82] Weeks, J. R.: *Real-time animation in hyperbolic, spherical, and product geometries*. A. Prékopa and E. Molnár, (eds.). Non-Euclidean Geometries, János Bolyai Memorial Volume, Mathematics and Its Applications, Springer Vol. 581, 287-305 (2006).

Affiliations

JENŐ SZIRMAI

ADDRESS: Department of Algebra and Geometry, Institute of Mathematics, Budapest University of Technology and Economics Műegyetem rkp. 3., H-1111 Budapest, Hungary.

E-MAIL: szirmai@math.bme.hu

ORCID ID:0000-0001-9610-7993